Tel1 Activation by the MRX Complex Is Sufficient for Telomere Length Regulation but Not for the DNA Damage Response in *Saccharomyces cerevisiae*

Rebecca Keener,*,† Carla J. Connelly,* and Carol W. Greider*,1
*Department of Molecular Biology and Genetics and †Biochemistry, Cellular and Molecular Biology Graduate Program, Johns Hopkins University School of Medicine, Baltimore, Maryland 21205
ORCID IDs: 0000-0001-9031-6866 (R.K.); 0000-0002-9218-5609 (C.J.C.); 0000-0002-5494-8126 (C.W.G.)

ABSTRACT Previous models suggested that regulation of telomere length in *Saccharomyces cerevisiae* by Tel1(ATM) and Mec1(ATR) would parallel the established pathways regulating the DNA damage response. Here, we provide evidence that telomere length regulation differs from the DNA damage response in both the Tel1 and Mec1 pathways. We found that Rad53 mediates a Mec1 telomere length regulation pathway but is dispensable for Tel1 telomere length regulation, whereas in the DNA damage response, Rad53 is regulated by both Mec1 and Tel1. Using epistasis analysis with a Tel1 hypermorphic allele, Tel1-hy909, we found that the MRX complex is not required downstream of Tel1 for telomere elongation but is required downstream of Tel1 for the DNA damage response. Our data suggest that nucleolytic telomere end processing is not a required step for telomerase to elongate telomeres.

KEYWORDS Tel1; MRX complex; telomere; DNA damage response; epistasis

TELOMERE length regulation is critical for cell viability and disruption of length homeostasis leads to disease (Stanley and Armanios 2015). Telomerase adds telomere repeats onto chromosome ends and redundant pathways tightly regulate this addition. In humans, decreased telomerase activity causes short telomere syndromes (Armanios and Blackburn 2012), while telomerase activation promotes cancer growth (Greider 1999). Thus, understanding the feedback pathways for maintaining telomeres is critical to understanding disease.

The checkpoint kinases Tel1, the Ataxia Telangiectasia-Mutated (ATM) homolog, and Mec1, the Ataxia-Telangiectasia and Rad3-related (ATR) homolog, have roles in sensing DNA damage and maintaining telomeres around an equilibrium point in yeast (Ritchie *et al.* 1999) and in mammalian cells (Lee *et al.* 2015; Tong *et al.* 2015; de Lange 2018), yet their underlying mechanisms remain unclear. In *Saccharomyces cerevisiae*, *MEC1* and *TEL1* mutations shorten telomeres. *MEC1* is an essential gene as *mec1*Δ cells are not able to activate dNTP production (Zhao *et al.* 1998). *mec1*Δ cells survive only with codeletion of either *SML1* or *CRT1* (also called *RFX1*), and in *mec1*Δ *sml1*Δ or *mec1*Δ *crt1*Δ cells, dNTP production is increased (Gupta *et al.* 2013; Maicher *et al.* 2017). *mec1*Δ *sml1*Δ have telomeres similar to wild type, while *mec1*Δ *crt1*Δ have slightly shorter telomeres. This difference has been attributed to the fact that *SML1* and *CRT1* regulate different pathways of dNTP production (Maicher *et al.* 2017). *mec1-21* and *mec1-14*, Mec1 hypomorphic alleles, have telomeres slightly shorter than wild type (Ritchie *et al.* 1999; Longhese *et al.* 2000). While deletion of *SML1* is most commonly used to rescue *mec1*Δ lethality, several studies have suggested that *sml1*Δ may mask telomere shortening phenotypes (Ritchie *et al.* 1999; Longhese *et al.* 2000), and these studies conclude that the Mec1 hypomorph telomere shortening demonstrates a role for Mec1 in telomere length regulation. *TEL1* deletion results in a clear telomere shortening that is more extensive than any *MEC1* deletion or mutant, and a *TEL1 MEC1* double mutant has an additive effect on telomere shortening, suggesting the kinases regulate parallel pathways (Ritchie *et al.* 1999). Mec1 and Tel1 also both play a role in the DNA damage response, where Mec1 has the

doi: https://doi.org/10.1534/genetics.119.302713
Manuscript received June 25, 2019; accepted for publication October 17, 2019; published Early Online October 23, 2019.
Supplemental material available at figshare: https://doi.org/10.25386/genetics.10029161.
[1]Corresponding author: Johns Hopkins University School of Medicine, 725 N. Wolfe St., Baltimore, Maryland 21205. E-mail: cgreider@jhmi.edu

greater effect. *TEL1* deletion on its own does not show DNA damage sensitivity, but *TEL1 MEC1* double mutants show higher sensitivity to DNA damage than *MEC1* mutants alone (Morrow *et al.* 1995). These experiments indicate that *TEL1* and *MEC1* have parallel roles in both telomere length regulation and the DNA damage response.

The distinct effects of *tel1*Δ and *mec1*Δ on telomere length and the DNA damage response suggest Tel1 and Mec1 may have different critical substrates. Both Tel1 and Mec1 phosphorylate proteins on serines and threonines at S/T-Q motifs (Kim *et al.* 1999). This identical phosphorylation motif has made identifying unique substrates of each kinase challenging. Mass spectrometry approaches have identified specific Tel1 and Mec1 substrates, in addition to shared substrates (Bastos de Oliveira *et al.* 2015), but the biological consequences of these phosphorylation events remain unclear.

While hundreds of Tel1/Mec1 substrates have been identified, those that are critical for telomere length have not been defined. We investigated the role of two known substrates, Rad53 and the Mre11-Rad50-Xrs2 (MRX) complex, which have been shown to be phosphorylated by Tel1 and/or Mec1 in response to DNA damage (D'Amours and Jackson 2001; Nakada *et al.* 2003b; Smolka *et al.* 2007; Albuquerque *et al.* 2008; Bastos de Oliveira *et al.* 2015; Lavin *et al.* 2015). In the DNA damage response, both Tel1 and Mec1 phosphorylate Rad53, activating its kinase activity (Figure 1A) (Lee *et al.* 2003; Nakada *et al.* 2003b). However, Tel1 phosphorylation of Rad53 is considered less important relative to Mec1 phosphorylation of Rad53 (Usui *et al.* 2001). In response to a double-strand break, Tel1 interaction with the MRX complex activates Tel1 kinase activity and Tel1 subsequently phosphorylates all three components of the MRX complex, in addition to other substrates (D'Amours and Jackson 2001; Nakada *et al.* 2003b; Smolka *et al.* 2007; Albuquerque *et al.* 2008; Lee *et al.* 2013; Bastos de Oliveira *et al.* 2015; Lavin *et al.* 2015). The process of end resection is complex and while the MRX complex is thought to initiate it, additional nucleases including Sae2 and Exo1 play important roles. Sae2 modulates Mre11 nuclease activity but is also thought to independently contribute to end resection (Arora *et al.* 2017). Exo1 extends the end resection and both Exo1 and Mre11 nuclease activities are required for optimal double-strand-break repair (Garcia *et al.* 2011). Several studies indicate that Tel1 modulates the MRX complex during this process, but it is unclear whether Tel1 phosphorylation of the MRX complex contributes to these regulatory mechanisms (Lavin *et al.* 2015). In this model, the MRX complex can be considered both upstream and downstream of Tel1 for the DNA damage response (Figure 1A). Several studies have suggested that similar regulatory events occur at telomeres (Nugent *et al.* 1998; Tsukamoto *et al.* 2001; Larrivee *et al.* 2004; Viscardi *et al.* 2007; Bonetti *et al.* 2009), although specific mechanisms are not well established.

In this study, we used mutagenesis and epistasis analysis and found that *RAD53* acts only in the *MEC1* telomere length pathway, not in the *TEL1* pathway. In addition, epistasis analysis showed the MRX complex acts both upstream and downstream of Tel1 in the DNA damage response, as characterized by others. However, strikingly, the MRX complex is only required upstream of Tel1 in telomere length regulation. Therefore, while the MRX complex is required to activate Tel1 kinase activity, it is not required for telomere resection. These findings demonstrate that the regulation of the MRX complex in the DNA damage response are distinct from their regulation in telomere length maintenance and challenge the assumption that a telomere must be resected for telomere elongation by telomerase.

Materials and Methods

Molecular cloning

Each plasmid was constructed using Gibson Assembly (Gibson 2011); for detailed explanations of cloning strategies, see Supplemental Material, File S1. Primers were designed using Snapgene software (GSL Biotech), products were amplified with Phusion HS II DNA polymerase (F549; Thermo Fisher), and Gibson Assembly Master Mix (E5510; New England Biolabs, Beverly, MA) was used according to the New England Biolabs recommended protocol. All restriction enzymes and NEB5α competent cells (C2987H) were from New England Biolabs. Plasmids were prepared using QIAprep Miniprep Kit (27106; Qiagen, Valencia, CA) and all sequencing was performed using the Sanger method.

Site-directed mutagenesis

S/T-Q mutations and *TEL1-hy909* mutations were introduced by site-directed mutagenesis using primers designed by PrimerX.org. Primer sequences are listed in Table S3. In each case, the plasmid was amplified using PfuTurbo (600252; Agilent). The product was *Dpn*I-treated, ethanol-precipitated, and transformed into DH5α cells (18265017; Thermo Fisher). Clones were isolated and sequence-verified.

Yeast culturing and transformation

Yeast culturing, transformation, and sporulation were conducted as previously described (Green and Sambrook 2012). Briefly, transformation was carried out on 50 ml of logarithmically cultured cells treated with 0.1 M lithium acetate (L6883; Sigma, St. Louis, MO). DNA was added to a 50 μl aliquot of cells in addition to 50 μg boiled fish sperm carrier DNA (11467140001; Roche). Cells were equilibrated at 30° for 10 min, after which 0.5 ml 40% polyethylene glycol (PEG_{4000}, P4338; Sigma) containing 0.1 M lithium acetate was added. Cells were incubated at 30° for 30 min then heat-shocked at 42° for 15 min. Transformed cells were washed with sterile water and plated on the appropriate selective media. In cases where an antibiotic selectable marker was used, cells were recovered in 1 ml yeast extract, peptone, dextrose (YPD) at 30° for 3–4 hr before plating. One-step integration was used for all integrated constructs. After transformation, integration at the desired locus was confirmed by junction polymerase chain reaction. In cases where

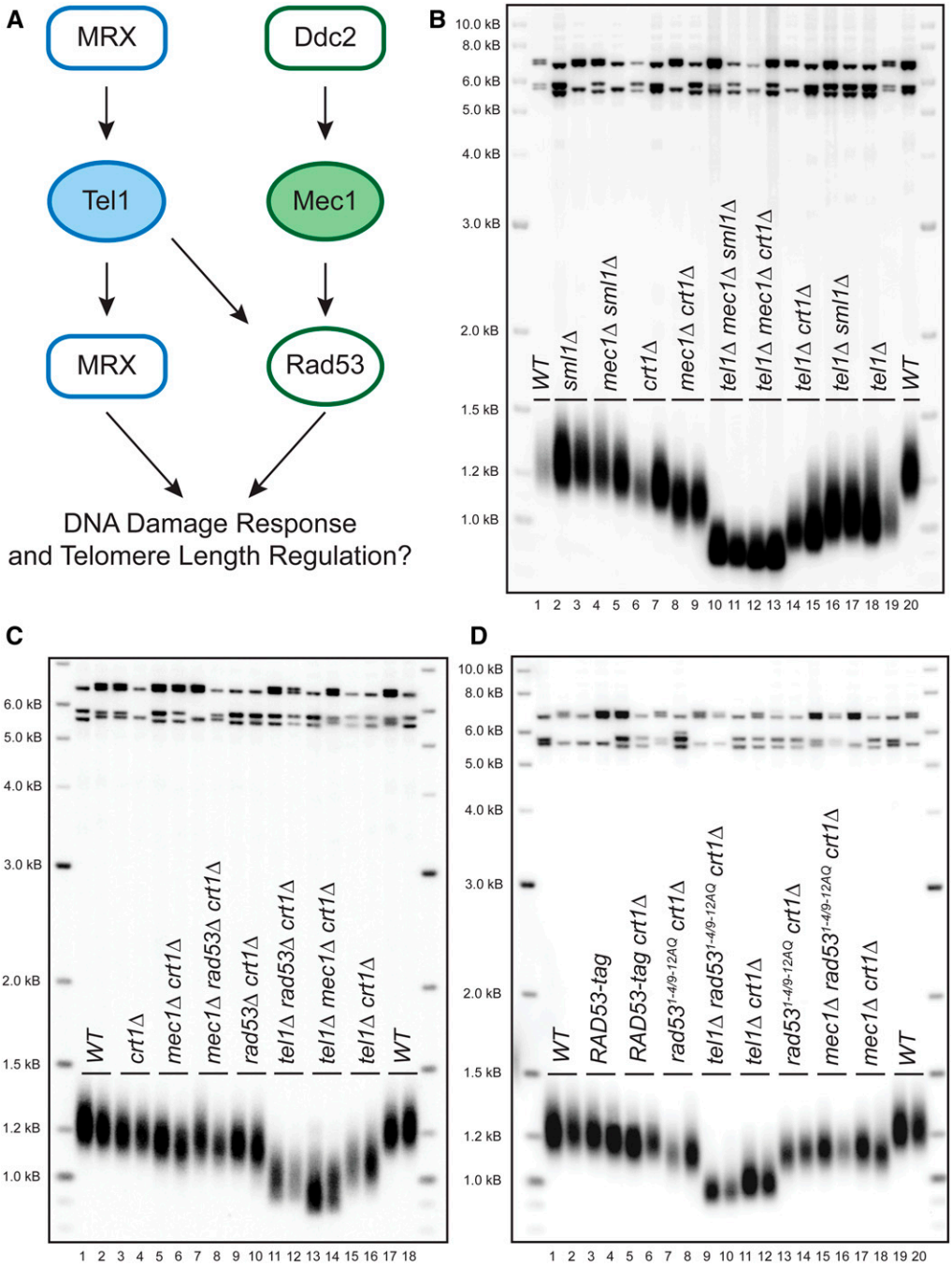

Figure 1 Rad53 is in the Mec1 telomere length regulation pathway. (A) Diagram representing a simplified, current understanding of Tel1/Mec1 pathways in the DNA damage response. (B–D) Southern blot analysis of telomeres from segregants with the indicated genotype. Two independent, haploid segregants are shown for each genotype. Median telomere length is quantitated in Figure S1, A–C. (B) Haploid cells were passaged on solid media for ~120 population doublings to decrease telomere length heterogeneity. Segregants are from JHUy937-1. Two biological replicates were assayed after 120 population doublings for each genotype. (C) Segregants are from yRK6002 and yRK6003. (D) Both Rad53 and rad53$^{1-4/9-12AQ}$ are epitope tagged with a 3xFLAG tag. Haploids were passaged for ~100 population doublings. Segregants are yRK6008-1, yRK6008-2, yRK6009-1, yRK6009-2, yRK6010-1, yRK6010-2, yRK6011-1, yRK6011-2, yRK6012-1, yRK6012-2, yRK6013-1, yRK6013-2, yRK6014-1, yRK6014-2, yRK6015-1, and yRK6015-2.

mutations were introduced, the region was amplified using Phusion HS II DNA polymerase, the amplicon was purified using AMPure beads (A63881; Beckman Coulter, Fullerton, CA), and sequenced to confirm the presence of mutations *in vivo*.

Passaging yeast

Because we initiate our experiments with strains that are heterozygous for multiple alleles of interest, dissection of 20 tetrads often yields all combinations of the alleles. This makes it possible to obtain experimental and control samples in parallel. Treating all haploids in parallel is critical for evaluating telomere length as telomere length can be sensitive to differences in culturing time. In cases where the diploid genotype did not allow isolation of an important control, a second diploid, from which that control can be segregated, was dissected in parallel. After tetrad dissection and replica plating to identify segregants of interest, haploids were streaked to single cell on a YPD plate. This streak was designated as the first passage and these cells are estimated to have undergone 40 population doublings. In experiments where cells were passaged, cells were restreaked on YPD plates repeatedly to increase the number of cell divisions. Each passaged plate was incubated for 48 hr at 30°, after which

cells were picked from the streak dilution and restreaked to single cell again on a fresh plate. Each passage is estimated to require ~20 population doublings. Therefore, a strain passaged five times undergoes a total of ~120 population doublings. At the desired number of passages, cells were inoculated into a 5 ml liquid YPD culture and grown at 30° overnight or until saturated. Cell pellets were saved at −20° until all time points had been collected, at which time genomic DNA was extracted. Images of the plates at specific time points were taken to document potential growth defects.

MRX-tag and mrx-18A strain construction

An yRK1006 *MRE11-3HA-URA3* segregant was mated to an yRK2040 *RAD50-G6-V5-LEU2* segregant, yielding yRK1. The *XRS2-13myc-hphMX4* construct (pRK1028) was transformed into yRK1, yielding yRK60. A *MRX-tag* haploid (yRK60 segregant) was mated to a *mec1*Δ *sml1*Δ haploid (JHUy816 segregant) to yield yRK79 and yRK80. The *mrx-18A* parental diploids were constructed in a manner parallel to the *MRX-tag* parental diploids. A yRK1052 *mre11-4A-3HA-URA3* segregant was mated to a yRK2082 *rad50-10A-G6-V5-TRP1* segregant, yielding yRK26. The *xrs2-4A-13myc-hphMX4* construct (pRK1040) was transformed into yRK26, yielding yRK56. A *mrx-18A* haploid (yRK56 segregant) was mated to a *mec1*Δ *sml1*Δ haploid (yYM242 segregant) to yield yRK81 and yRK83. Mutations were confirmed again in yRK81 and yRK83 by sequencing.

rad50S knock-in using CRISPR/Cas9

Guide RNA sequences were chosen using the algorithms published by Doench *et al.* via the Benchling (Biology Software 2019) interface (Doench *et al.* 2016). Two guides, RW 670 and RW 671, were individually cloned into pCAS026 using the strategy described previously (Anand *et al.* 2017). Guide RNA sequences are listed in Table S3. Double-stranded homology repair templates were amplified (primers RW 674 and RW 675) using a 90-mer oligonucleotide as the template. The repair template was designed to both introduce the rad50S mutation (Lys81Ile) (Alani *et al.* 1990) and introduce a silent mutation in the protospacer adjacent motif sequence. The 90-mer oligonucleotide RW 672 was used as the template for the RW 670 guide and 90-mer oligonucleotide RW 673 was used as the template for the RW 671 guide. Solid Phase Reversible Immobilization beads (B23318; Beckman Coulter) were used to purify the repair template before transformation. yRK114 haploid cells were cultured for transformation as described above, except that no carrier DNA was added and 100 μl of cells were used in the transformation reaction. Cells were transformed with 1 μg of pCAS026 containing the appropriate guide and 4–5 μg of double-stranded repair template. Cells were grown on minimal media without uracil to select for cells that contained the pCAS026 plasmid. The *rad50S* allele was validated by sequencing. yRK2112 was edited using the RW 670 guide, while yRK2116 was edited using the RW 671 guide. yRK2113 was transformed with pCAS026 containing the RW 670 guide but was not edited and was used in parallel to serve as a control. Haploids were streaked on minimal media containing 5-fluoroorotic acid (F595000; Toronto Research Chemicals) to select against the pCAS026 plasmid, followed by five passages on YPD plates before telomere elongation was observed by Southern blot (data not shown).

Southern blots and quantitative analysis

Genomic DNA was extracted and used for Southern blot analysis as described previously (Kaizer *et al.* 2015). Briefly, a cell pellet of ~50 μl was resuspended in 1× lysis buffer (10 mM Tris, pH 8.0, 0.5 M EDTA, pH 8.0, 100 mM NaCl, 1% SDS, 2% Triton X-100) and cells were lysed in the presence of 0.5 mm glass beads (11079105; Biospec Products). Phenol-chloroform (50:50) was added and cells were vortexed for 8 min (Eppendorf mixer 5432). The DNA was ethanol precipitated and resuspended in 40–50 μl TE (10 mM Tris, pH 8.0, 1 mM EDTA) with RNaseA (R6513, 10 μg/ml; Sigma) at 37° for 1 hr or 4° overnight.

Samples were cut with the restriction enzyme *Xho*I and electrophoresed at 47 V (12 mA) on a 1.0% agarose in 1× TTE buffer (20x = 1.78 M Tris base, 0.57 M taurine, 0.01 M EDTA) for ~24 hr. A total of 200 ng of two-log DNA ladder (N3200; New England Biolabs) was included for reference. The genomic DNA was transferred to a Hybond N+ membrane (RPN303B; GE Healthcare) by vacuum blotting (Boekel Appligene vacuum blotter) for 1 hr at 50 mbar with the gel covered in 10× SSC buffer (1.5 M NaCl, 0.17 M sodium citrate). Once transferred, the DNA was UV cross-linked (UV Stratalinker 2400; Stratagene, La Jolla, CA). The membrane was prehybridized in Church buffer (0.5 M Tris, pH 7.2, 7% SDS, 1% bovine serum albumin, 1 mM EDTA) at 65°, then α^{32}P-dCTP–radiolabeled (Perkin Elmer, Norwalk, CT) fragments of the Y' element and the two-log DNA ladder were added at 10^6 cpm/ml and 10^4 cpm/ml, respectively. The membrane was incubated with the radiolabeled probe overnight, washed in 1× SSC, 0.1% SDS buffer at 65°, imaged with a Storage Phosphor Screen (GE Healthcare) overnight, and then scanned on a Storm 825 imager (GE Healthcare). The images were copied from ImageQuant TL (GE Life Sciences) to Adobe PhotoShop CS6 and saved as .tif files. The images were cropped in Adobe PhotoShop CS6 to show both internal Y' elements at the top and the telomere restriction fragment (TRF) band.

Telomere length was quantified in ImageQuant TL. The median TRF length was measured as the point of highest intensity in the Y' telomere fragment distribution. The length in base pairs was determined by comparison to the two-log DNA ladder. Where possible, ladders were loaded in multiple wells across the gel to account for minor differences in migration. The length of each TRF was normalized to the length of the wild-type sample in the same gel. In cases where the same wild-type sample was run on the Southern blot multiple times, the average is reported. Samples were only considered biological replicates if they had been passaged the same

number of times as passaging may affect telomere length. Data were graphed using GraphPad Prism 5.0b. An unpaired two-tailed Student's *t*-test was performed between samples to determine statistical significance.

Western blots

Protein extracts were prepared by trichloroacetic acid extraction (Link and LaBaer 2011). Samples were resolved on a NuPAGE 3–8% Tris-Acetate gradient polyacrylamide gel (EA0375; Invitrogen, Carlsbad, CA) in 1× Tris-Acetate running buffer (LA0041; Invitrogen) using the Invitrogen NuPAGE system with protein ladder standards (161-0374; Bio-Rad, Hercules, CA). The gel was transferred by electroblotting to a PVDF membrane (IPFL00010; Thermo Fisher) using NuPAGE transfer buffer (20x: 40.8 g bicine, 52.4 g Bis-Tris, 3.0 g EDTA) at 30 V for 1.5 hr. The membrane was blocked with Odyssey buffer (Li-Cor 927–40000) for 1 hr at room temperature or overnight at 4°. Primary antibodies were diluted in blocking buffer and incubated at room temperature for 1 hr [Sigma-Aldrich M2 Flag at 1:1000 (Sigma-Aldrich); 22C5D8 Pgk1 at 1:6000 (Invitrogen); 12CA5 HA at 1:2000 (Roche); R960-25 V5 at 1:2000 (Invitrogen); and 9E10 c-myc at 1:10,000 (Santa Cruz Biotechnology)]. The membrane was washed in 1× Tris-buffered saline with Tween-20 (TBST) buffer (10x TBST: 0.2 M Tris base, 1.5 M NaCl, 0.1% Tween-20) before incubation at room temperature for 30 min with a horseradish peroxidase–conjugated secondary antibody (1706516; Bio-Rad at 1:10,000) in 5% powdered milk (170-6404; Bio-Rad) resuspended in 1× TBST. The membrane was washed in 1× TBST and then incubated with Forte horseradish peroxidase substrate (WBLUF0100; Millipore, Bedford, MA) followed by imaging on ImageQuant LAS 4000 mini biomolecular imager (GE Healthcare). The images were copied from ImageQuant to Adobe PhotoShop CS6 and saved as .tif files. Western blots were quantified using ImageQuant TL. The pixel volume was calculated for each band using boxes of fixed size across the blot. The volume for each sample was normalized to the Pgk1 volume for that lane and then taken as a ratio to the first tagged sample on the blot. Data were graphed using GraphPad Prism 5.0b. An unpaired two-tailed Student's *t*-test was performed between samples.

Mutagen challenge spotting assay

Strains of interest were inoculated to an initial OD600 of 0.15–0.25 in 8–10 ml YPD. Once the density reached an OD600 of 0.5–0.6, the culture was split into untreated and treated samples. 4-Nitroquinoline (N8141; Sigma) was resuspended in acetone at a stock concentration of 1 mM. Bleomycin (15U, C103610; Fresenius Kabi) was dissolved in 10 ml sterile water and used as a 1 mg/ml stock. Hydroxyurea (H9120; US Biologicals) was resuspended in sterile water at a stock concentration of 1 M. Methyl methanesulfonate (MMS) (129925; Sigma) was treated as 100%. The appropriate chemical was added to each treated sample and cultured at 30° with slight agitation for 1–2 hr, as indicated in the figure legends. Untreated samples were cultured in parallel. Cell pellets of equal density were collected for each sample based on the OD600. The size of the cell pellet varied between experiments from 0.6 OD to 4.0 OD, as indicated in the figure legends. Each pellet was resuspended in 1 ml YPD and serially diluted 1:5 in YPD in a 96-well dish. A total of 4 μl of each dilution was spotted onto a YPD plate and the plates were cultured at 30° for 48 hr, before being imaged on a Bio-Rad Gel Doc XR+ Imaging System under white light, using Image Lab v6.0.1 software.

Quantitative MMS time-course survival assay

Freshly grown strains of interest were inoculated to an initial OD600 of 0.2–0.3 in 6 ml YPD. Once density reached 0.5–0.6 OD600, an untreated sample was plated for each strain before cells were treated with 0.01% MMS. Thirty-minute time points were taken up to 120 min for each strain. A Millipore Scepter with 40 μm tips was used to measure cells/ml at each time point. Approximately 500 cells were plated across five YPD plates, with ~100 cells per plate, for each strain and at each time point. Samples were blinded before plating and the plates were incubated at 30° for 48 hr. Colony forming units were counted for each blinded sample and once all plates were counted, the results were unblinded. At each time point the number of colonies was calculated as a proportion: the total number of colonies for that strain at that time point relative to the total number of colonies for that strain at the untreated time point ($t = 0$). Data were graphed using GraphPad Prism 5.0b and the SE of the mean is shown.

Plasmid end-joining assay

Cells were cultured and treated as described above for yeast transformation. Once density reached an OD600 of 0.6–0.8 the cells were transformed with 100 ng of *Stu*I-linearized pRS317 (Sikorski and Boeke 1991), which generates blunt ends, or with 100 ng of circular pRS317. A total of 50 μg boiled fish sperm carrier DNA (11467140001; Roche) was added to both linear and circular transformation reactions. Three replicate transformations were performed for both linear and circular plasmids for each strain. Samples were blinded and cells were plated on minimal media without lysine. After 48 hr of incubation at 30°, colony forming units were counted. Once all plates were counted, samples were unblinded. The average number of colonies of the three replicates containing circular DNA was calculated for each strain. Each linear DNA transformation was treated as a technical replicate. The number of colonies from each linear DNA transformation plate was normalized to the average number of colonies of circular DNA for that strain. Data were plotted and analyzed in GraphPad Prism 5.0b. An unpaired two-tailed Student's *t*-test was performed between samples.

Data availability

All strains and plasmids are available upon request. Table S1 contains all strains used in this study. Table S2 contains all plasmids used in this study and a brief description of their

purpose. Table S3 contains all primers used in this study and a brief description of their purpose. Table S4 is the reagent table for this study and provides a reference for all genes, strains, software, and many reagents used in this study. File S1 has a detailed explanation of how all plasmids used in this study were constructed. Supplemental material available at figshare: https://doi.org/10.25386/genetics.10029161.

Results

Rad53 regulates telomere length through the Mec1 pathway

Rad53 kinase is a candidate substrate that could mediate telomere length, since both Tel1 and Mec1 phosphorylate Rad53 (Nakada *et al.* 2003b) and *RAD53* mutants show telomere shortening (Longhese *et al.* 2000). We used epistasis and mutational analyses to examine whether Rad53 functions in the Tel1 or Mec1 telomere length pathway (Figure 1A). We deleted either *SML1* or *CRT1*, regulators of dNTP pools that were previously shown to suppress the lethality of *mec1*Δ and *rad53*Δ (Huang *et al.* 1998; Zhao *et al.* 1998). While it is most common in the literature to use *sml1*Δ to rescue *mec1*Δ lethality, there is evidence that *SML1* deletion can mask telomere length phenotypes (Ritchie *et al.* 1999; Longhese *et al.* 2000). Therefore, we initially compared the effects of deleting *sml1*Δ or *crt1*Δ on telomere length in *tel1*Δ or *mec1*Δ mutants.

All of our experiments were carried out in haploid yeast; however, to avoid telomere length changes that can occur with long term propagation of haploids, we standardly generated fresh haploids by sporulating heterozygous diploids (see *Materials and Methods*). We generated diploid strains that were heterozygous for *TEL1/tel1*Δ, *MEC1/mec1*Δ, *SML1/sml1*Δ, and *CRT1/crt1*Δ and then sporulated to obtain haploids with specific mutant combinations. To quantitate subtle telomere length differences, we measured the median TRF length relative to the wild-type sample in the same Southern for multiple replicates of the same genotype (see *Materials and Methods*). While *sml1*Δ (0.994) cells and *mec1*Δ *sml1*Δ (0.968) cells had telomeres not significantly different from wild-type cells ($P > 0.05$), *crt1*Δ cells had slightly shorter telomeres (0.912) than wild-type cells, and *mec1*Δ *crt1*Δ telomeres were significantly shorter (0.875) ($P = 0.0440$) (Figure 1B, compare lanes 2–5 to lanes 6 and 7 and to lanes 8 and 9; quantitation in Figure S1A). *mec1*Δ *crt1*Δ telomeres were similar to the shorter telomeres reported in *mec1-14* and *mec1-21* cells (Ritchie *et al.* 1999; Longhese *et al.* 2000). While *tel1*Δ *sml1*Δ cells showed short telomeres (0.826) that were not significantly different from *tel1*Δ mutants (0.827) ($P > 0.05$), *tel1*Δ *crt1*Δ telomere lengths appear even shorter (0.767) than *tel1*Δ *sml1*Δ, although were not statistically distinct from *tel1*Δ ($P > 0.05$) (Figure 1B, compare lanes 14 and 15 to lanes 16 and 17 to lanes 18 and 19; quantitation in Figure S1A). We conclude that *sml1*Δ masks the short telomere phenotype of *mec1*Δ cells, as shown previously (Ritchie *et al.* 1999; Longhese *et al.* 2000). However, *crt1*Δ does not, although it does have a mild telomere shortening effect on its own.

To examine whether Rad53 plays a role in the Tel1 or Mec1 telomere length pathway, we generated diploids heterozygous for *TEL1/tel1*Δ, *MEC1/mec1*Δ, *RAD53/rad53*Δ, and *CRT1/crt1*Δ and sporulated to obtain specific mutant combinations. We observed that *crt1*Δ suppresses *rad53*Δ lethality, consistent with previous reports (Figure S2B) (Huang *et al.* 1998). We compared *mec1*Δ *crt1*Δ telomeres (0.965) to *mec1*Δ *rad53*Δ *crt1*Δ telomeres (0.959). There was no apparent additive shortening and no significant difference ($P > 0.05$) between the median TRF length (Figure 1C, compare lanes 5 and 6 to lanes 7 and 8; quantitation in Figure S1B), which is consistent with Rad53 functioning in the Mec1 telomere length regulation pathway. In contrast, we found there was additive shortening when we compared *tel1*Δ *rad53*Δ *crt1*Δ telomeres (0.839) to *tel1*Δ *crt1*Δ telomeres (0.888), where *tel1*Δ *rad53*Δ *crt1*Δ telomeres were significantly shorter ($P = 0.0112$) (Figure 1C, compare lanes 11 and 12 to lanes 15 and 16; quantitation in Figure S1B), supporting the conclusion that Tel1 and Rad53 are in different length regulation pathways. However, *tel1*Δ *rad53*Δ *crt1*Δ telomeres (0.839) were slightly, but significantly ($P = 0.0111$), longer than *tel1*Δ *mec1*Δ *crt1*Δ telomeres (0.795) (Figure 1C, compare lanes 11 and 12 to lanes 13 and 14; quantitation in Figure S1B), suggesting that either Rad53 has functions in both the Tel1 and Mec1 telomere length pathways or that Rad53 acts exclusively in the Mec1 telomere length pathway which also relies on additional Mec1 substrates for telomere length regulation.

Phosphorylation of Rad53 on S/T-Q motifs regulates telomere length

To examine the role of Rad53 as a Tel1/Mec1 substrate that mediates telomere length, we examined a Rad53 mutant where Tel1/Mec1 S/T-Q phosphorylation motifs were mutated to A-Q. Previous work demonstrated that a subset of the Rad53 S/T-Q motif clusters are critical for Rad53 function in the DNA damage response and that this mutant, $rad53^{1-4/9-12AQ}$, could not respond to Mec1 or Tel1 regulation (Lee *et al.* 2003). Both Rad53 and $rad53^{1-4/9-12AQ}$ were viable when expressed off of a plasmid using the endogenous promoter in *rad53*Δ cells and did not require codeletion of *SML1* or *CRT1* (Figure S3A and data not shown). We integrated 3xFLAG-tagged $rad53^{1-4/9-12AQ}$ or 3xFLAG-tagged *RAD53* at the endogenous locus in *TEL1/tel1*Δ, *MEC1/mec1*Δ, *CRT1/crt1*Δ diploid cells to better control the segregation of these alleles. Rad53 and $rad53^{1-4/9-12AQ}$ were stably expressed, as shown previously (Lee *et al.* 2003) (data not shown). Unlike the plasmid expression system, we noted that integrated $rad53^{1-4/9-12AQ}$ is lethal unless it cosegregates with *sml1*Δ or *crt1*Δ (Figure S3B). While the *RAD53-tag* cells had slightly shorter telomeres (0.977) than wild type, there was additional shortening in $rad53^{1-4/9-12AQ}$ *crt1*Δ cells (0.911) compared to *RAD53-tag* *crt1*Δ cells (0.946) (Figure 1D, compare lanes 7 and 8 to

lanes 5 and 6; quantitation in Figure S1C), demonstrating that phosphorylation of Rad53 contributes to telomere length regulation.

We did not observe additive shortening in *mec1*Δ *rad53*$^{1-4/9-12AQ}$ *crt1*Δ cells (0.922) compared to *mec1*Δ *crt1*Δ cells (0.916) or *rad53*$^{1-4/9-12AQ}$ *crt1*Δ cells (0.911) (Figure 1D, compare lanes 15 and 16 to lanes 17 and 18 and lanes 13 and 14; quantitation in Figure S1C), consistent with Mec1 targeting these phosphorylation sites. In contrast, we observed additive shortening in *tel1*Δ *rad53*$^{1-4/9-12AQ}$ *crt1*Δ cells (0.775) compared to *rad53*$^{1-4/9-12AQ}$ *crt1*Δ cells (0.911) or to *tel1*Δ *crt1*Δ cells (0.804) (Figure 1D, compare lanes 9 and 10 to lanes 7 and 8 and to lanes 11 and 12; quantitation in Figure S1C), further supporting the conclusion that Tel1 and Rad53 are in different pathways. This additive telomere shortening suggests that Rad53 is primarily in the Mec1 telomere length pathway.

Tel1-hy909 requires Rad53 for DNA damage response but not for telomere length regulation

To directly examine whether Tel1 telomere length regulation is Rad53-dependent, we performed epistasis analysis with *rad53*Δ *crt1*Δ and a Tel1 hypermorphic allele, *TEL1-hy909*, which has increased Tel1 kinase activity, increased DNA damage response function, and long telomeres (Baldo *et al.* 2008). We generated diploids heterozygous for *TEL1/TEL1-hy909*, *RAD53/rad53*Δ, and *CRT1/crt1*Δ and diploids heterozygous for *TEL1/TEL1-hy909*, *MEC1/mec1*Δ, and *CRT1/crt1*Δ. We first examined the DNA damage response in haploid cells by challenging them with a DNA-damaging agent, MMS. Consistent with previous data, *mec1*Δ *crt1*Δ cells were sensitive to DNA damage while *TEL1-hy909 mec1*Δ *crt1*Δ cells were not (Figure 2A) (Baldo *et al.* 2008). This indicates that the Tel1 hypermorph can rescue the DNA damage response in a *mec1*Δ mutant. Like *mec1*Δ *crt1*Δ, the *rad53*Δ *crt1*Δ cells were also sensitive to DNA damage (Figure 2B). However, unlike *TEL1-hy909 mec1*Δ *crt1*Δ cells, *TEL1-hy909* rad53Δ *crt1*Δ cells were still sensitive to MMS challenge (Figure 2B). Further, while *TEL1-hy909* was able to rescue *mec1*Δ lethality (Figure S2B), as previously shown (Baldo *et al.* 2008), *TEL1-hy909* was not able to rescue *rad53*Δ lethality (Figure S2A). Western blot analysis showed that there were similar levels of the 2xFlag-tagged Tel1-*hy909* in *TEL1-hy909 crt1*Δ cells, *TEL1-hy909 mec1*Δ *crt1*Δ cells, and *TEL1*-hy909 *rad53*Δ *crt1*Δ cells (Figure S4A). These data indicate that Rad53 mediates the Tel1-*hy909* DNA damage response.

We next examined telomere length in *TEL1-hy909* and *TEL1-hy909 rad53*Δ *crt1*Δ mutants. *TEL1-hy909 rad53*Δ *crt1*Δ cells initially had an intermediate telomere length between *TEL1-hy909* and *rad53*Δ *crt1*Δ (Figure 2C). This indicates that either Rad53 has a partially redundant role in the Tel1 telomere length regulation pathway or that Rad53 and Tel1 function in independent pathways. We noted that independent segregants had variable telomere lengths (Figure 2C, compare lanes 5 and 6). Indeed, even the wild-type telomeres were heterogeneous (Figure 2C, lanes 1, 2, 9, and 10). The *TEL1-hy909* allele was reported to be dominant to Mec1 in the DNA damage response (Baldo *et al.* 2008). Therefore, we were not surprised to observe that *TEL1-hy909* has a dominant effect on telomere length as *TEL1/TEL1-hy909* parental diploids have significantly longer telomeres than *TEL1/TEL1* diploids (Figure S4B). We attribute the differences observed in independent haploid segregants to clonal effects generated by segregation from a very heterogeneous telomere population in the *TEL1-hy909* parental diploid. Because each segregant begins as a single cell, the initial telomeres length could start anywhere along the wide telomere length distribution. Thus, the new length distribution is established at a slightly different midpoint for each clone. This phenomenon of clonal variation in telomere distributions was previously described (Shampay and Blackburn 1988), and is greatly exacerbated in long telomere mutants. To reduce the clonal variation and examine the effect of Rad53, we passaged cells for ~120 population doublings and repeated the Southern blot. Because of the clonal variation, extensive telomere length variance, and easily apparent effects on telomere length, we did not use quantification in experiments with *TEL1-hy909*. We reasoned that if Rad53 was important for Tel1-hy909 telomere elongation then telomeres would not further elongate with increased divisions in the absence of Rad53. However, we observed that in *TEL1-hy909 rad53*Δ *crt1*Δ passaged cells, telomeres elongated from passage 1 to passage 5 (Figure 2D, compare lanes 9 to 11 and 10 to 12) and the variability in *rad53*Δ *crt1*Δ cells was reduced (Figure 2D, compare lanes 5 to 7 and 6 to 8). This suggests that Rad53 is not required for Tel1-hy909 telomere lengthening, which is in stark contrast to the Rad53 dependence of Tel1-hy909 for the DNA damage response (Figure 2B). Together, these data suggest that Rad53 functions in the Mec1 telomere length pathway, but is not required in the Tel1 telomere length pathway.

S/T-Q sites in MRX are not required for DNA damage response or telomere length regulation

Having found that Rad53 is not essential to mediate the Tel1 telomere length response, we next tested whether the MRX complex might be a critical Tel1 substrate. In both yeast and mammalian cells, all three components of the MRX(N) complex are phosphorylated by Tel1/Mec1 (ATM/ATR) (D'Amours and Jackson 2001; Nakada *et al.* 2003b; Smolka *et al.* 2007; Albuquerque *et al.* 2008; Bastos de Oliveira *et al.* 2015; Lavin *et al.* 2015). Tel1 and Mec1 have a well-characterized and conserved S/T-Q phosphorylation motif (Kim *et al.* 1999). Previous work showed that mutation of all S/T-Q motifs in Xrs2 to A-Q had no effect on the DNA damage response or on telomere length (Mallory *et al.* 2003). To further probe whether MRX phosphorylation affects function, we mutated all S/T-Q motifs across the entire MRX complex and examined the effect on DNA damage response and telomere length.

Each MRX gene was epitope-tagged, the S/T-Qs were mutated to A-Qs, and the constructs were integrated at the

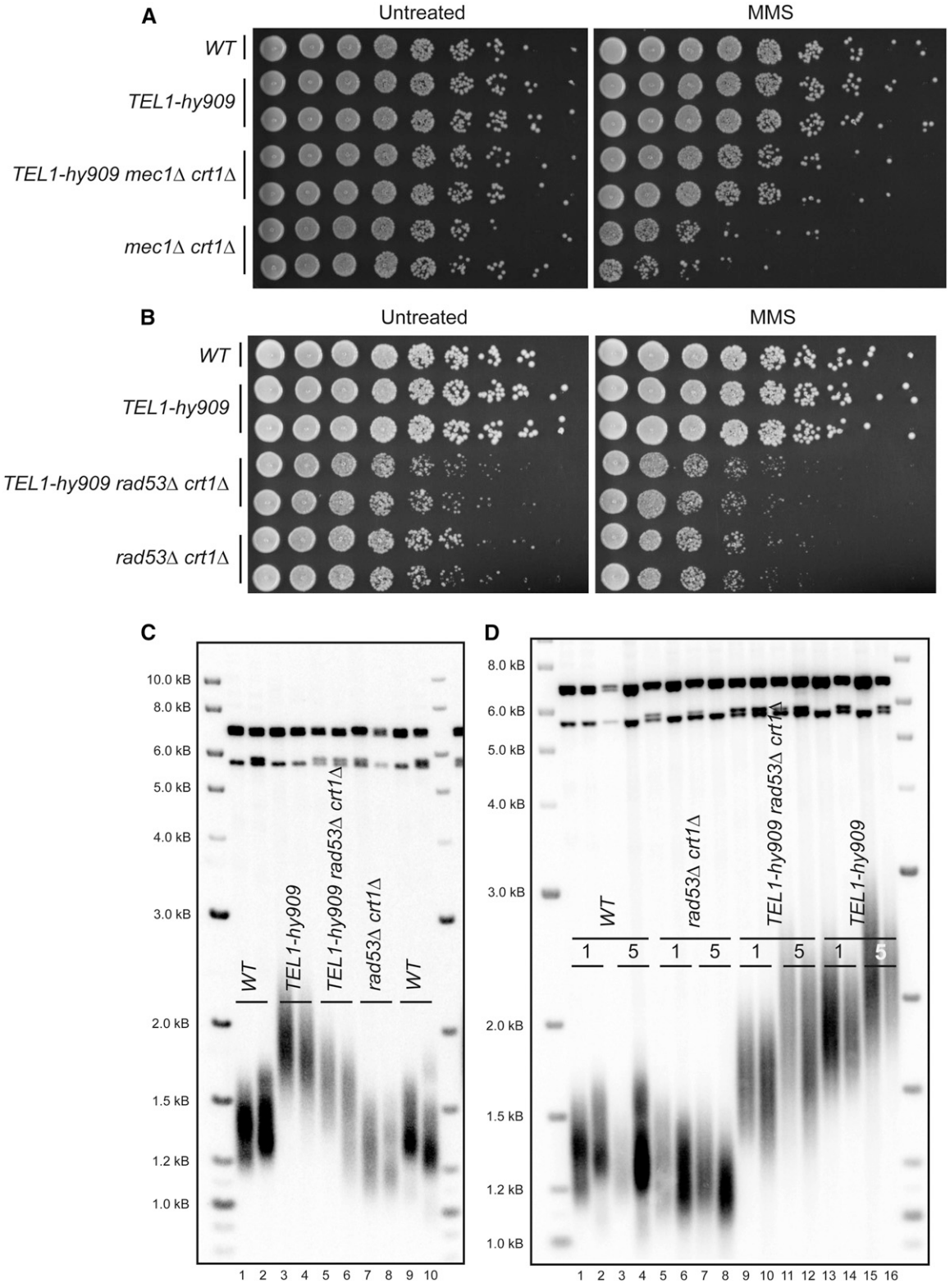

Figure 2 Tel1-hy909 requires Rad53 for the DNA damage response but not telomere elongation. (A and B) Yeast dilution series of untreated cells or cells cultured in 0.02% MMS for 1 hr. The genotype is indicated to the left of the panels. (A) Segregants are from yRK5126 and yRK5127. (B) Segregants are from yRK5028 and yRK5059. (C) Southern blot analysis of telomeres from segregants with the indicated genotype. Two independent, haploid segregants are shown for each genotype. Additional biological replicates were assayed for each genotype: *WT*, $n = 35$; *TEL1-hy909*, $n = 42$; *TEL1-hy909 rad53Δ crt1Δ*, $n = 6$; *rad53Δ crt1Δ*, $n = 5$. Because the *TEL1-hy909* hypermorph elongates telomeres in the parental diploid (Figure S4B), we observed increased telomere length heterogeneity across all genotypes in the haploid segregants and observe the wild-type segregant telomeres were longer compared to other Southern blots. Segregants are from yRK5028 and yRK5059. (D) Southern blot analysis of telomeres from segregants with the indicated genotype. Segregants were passaged on solid media for ~120 population doublings. Passage number is indicated: 1 = first passage or 5 = fifth passage. Segregants are from yRK5028. Additional biological replicates examined for P1 samples, see Figure 2C legend. Two biological replicates were assayed for each genotype at P5.

endogenous locus (Figure 3A). We generated three strains with each gene individually mutated at all S/T-Q sites, termed *mre11-4A*, *rad50-10A*, and *xrs2-4A*, as well as a strain containing all three mutants, termed *mrx-18A* (see *Materials and Methods*). As a control, we generated three strains in which each protein is epitope-tagged but has wild-type coding sequence and a strain which has all three MRX complex components epitope-tagged, referred to as *MRX-tag*. Individually, and in combination with one another, the altered proteins were stable as determined by Western blot, indicating that mutations do not affect protein stability (Figure 3B and Figure S5A).

To examine the role of Tel1 and Mec1 phosphorylation of MRX on the DNA damage response, we tested the *mrx-18A* mutant for MMS sensitivity. None of the MRX S/T-Q mutants individually or in combination showed increased sensitivity to MMS, hydroxyurea, bleomycin, or 4-nitroquinoline (Figure S5B and data not shown). We noted *tel1*Δ alone also does not have detectable MMS sensitivity (Figure S5B), but there is an observable increase in MMS sensitivity in *tel1*Δ *mec1*Δ *sml1*Δ compared to *mec1*Δ *sml1*Δ (Figure S5C). To take advantage of this increased sensitivity, we put *mrx-18A* and *MRX-tag* in the sensitized background of *mec1*Δ *sml1*Δ and assayed cells for an increased MMS sensitivity compared to *mec1*Δ *sml1*Δ alone.

Using the spotting assay, it was difficult to determine whether the sensitivity of *mrx-18A mec1*Δ *sml1*Δ cells was increased compared to *MRX-tag mec1*Δ *sml1*Δ cells (Figure S5C). To quantify the subtle DNA damage defect of *mrx-18A mec1*Δ *sml1*Δ cells we used a more sensitive time-course mutagen survival assay where colony forming units are counted after treatment with MMS for increasing lengths of time. In this quantitative assay we observed no difference in MMS sensitivity between *mrx-18A mec1*Δ *sml1*Δ cells compared to *MRX-tag mec1*Δ *sml1*Δ (Figure 3C). We also noted in this assay that *MRX-tag mec1*Δ *sml1*Δ cells were slightly more sensitive than *mec1*Δ *sml1*Δ, suggesting the tags have a small effect on MRX complex function (Figure 3C). The epitope tags do not greatly disrupt function as this small effect was only observed in a *mec1*Δ *sml1*Δ sensitized background. No increased sensitivity was observed by spotting assay in response to 4-nitroquinoline, bleomycin, or hydroxyurea (Figure S6, A–C). As a control, we also examined *mrx-18A tel1*Δ, and found no increased MMS sensitivity (Figure S6D).

In addition to its role in homology-directed repair, MRX also plays a critical role in nonhomologous end joining (NHEJ) in yeast (Moore and Haber 1996). We tested the effect of *mrx-18A* on NHEJ using a plasmid religation assay (Boulton and Jackson 1996), and found no effect of *mrx-18A* compared to *MRX-tag* (Figure 3D). These data suggest that phosphorylation of MRX on S/T-Q sites does not play a major role in NHEJ.

Individual mutant subunits, *mre11-4A*, *rad50-10A*, and *xrs2-4A*, telomere length was not significantly different ($P > 0.05$) from epitope-tagged controls (Figure 3E, quantitation in Figure S7A). We found *MRX-tag* cells (0.916) exhibited statistically significant ($P < 0.0001$) telomere shortening compared to untagged alleles (1.000), consistent with a slight defect seen in the DNA damage assay; however, *mre11*Δ telomeres (0.815) were significantly shorter by comparison ($P < 0.0001$). We next compared the telomere length phenotype of the *mrx-18A* (0.916) to *MRX-tag* telomere length (0.921) and found no significant effect ($P > 0.05$) (Figure 3F; quantitation in Figure S7B). To determine whether a change in telomere length would be seen after further cell divisions, we passaged *mrx-18A* cells for ~120 population doublings and still saw no significant effect on telomere length (Figure S7, C and D). These data suggest that phosphorylation of the MRX complex by Tel1 or Mec1 on S/T-Q sites is not critical for telomere length regulation.

MRX is required downstream of Tel1 for the DNA damage response but not telomere length

The lack of requirement for MRX phosphorylation by Tel1 or Mec1 raised the question of whether MRX is required downstream of Tel1. Because double mutants of either *mre11*Δ, *rad50*Δ, or *xrs2*Δ with *tel1*Δ produces a short telomere phenotype similar to any individual mutant, it is not possible to establish epistasis. Therefore, we performed epistasis analysis with the *TEL1-hy909* hypermorphic allele and *mre11*Δ, *rad50*Δ, or *xrs2*Δ. As described earlier, *TEL1-hy909* elongates telomeres and provides a stark contrast to the short telomeres in *mre11*Δ, *rad50*Δ, or *xrs2*Δ cells. Many studies have shown Tel1 and MRX act in the same pathway and Xrs2 has been shown to recruit Tel1 to double-strand breaks (Nakada *et al.* 2003a) and to telomeres (Hector *et al.* 2007; Sabourin *et al.* 2007). Current models of DNA repair indicate that MRX first recruits Tel1 to a DNA double-strand break and activates the kinase, Tel1 then phosphorylates MRX, and then MRX, with other nucleases, processes DNA ends for repair (Oh and Symington 2018; Paull 2018). Analogous pathways have been proposed for Tel1 and MRX in telomere length regulation, (Nugent *et al.* 1998; Tsukamoto *et al.* 2001; Viscardi *et al.* 2007; Bonetti *et al.* 2009) predicting that the MRX complex is downstream of Tel1 and that the MRX complex should be epistatic to Tel1 in both the DNA damage response and telomere length regulation.

To examine the epistasis of MRX and Tel1, we generated strains heterozygous for *TEL1/TEL1-hy909*, *MEC1/mec1*Δ, and *SML1/sml1*Δ together with individual heterozygous deletions of *mre11*Δ, *rad50*Δ, or *xrs2*Δ and initially examined the DNA damage response. We observed the *TEL1-hy909 mre11*Δ double mutants were as sensitive to MMS as *mre11*Δ alone (Figure 4A), consistent with previous work (Baldo *et al.* 2008). The other two double mutants, *TEL1-hy909 rad50*Δ and *TEL1-hy909 xrs2*Δ, were also both MMS-sensitive (not shown). These results support a role for MRX downstream of Tel1 in the DNA damage response, as previously reported (Moore and Haber 1996; Usui *et al.* 2001). We found that, surprisingly, *TEL1-hy909 mec1*Δ *mre11*Δ spores were inviable, indicating the rescue of

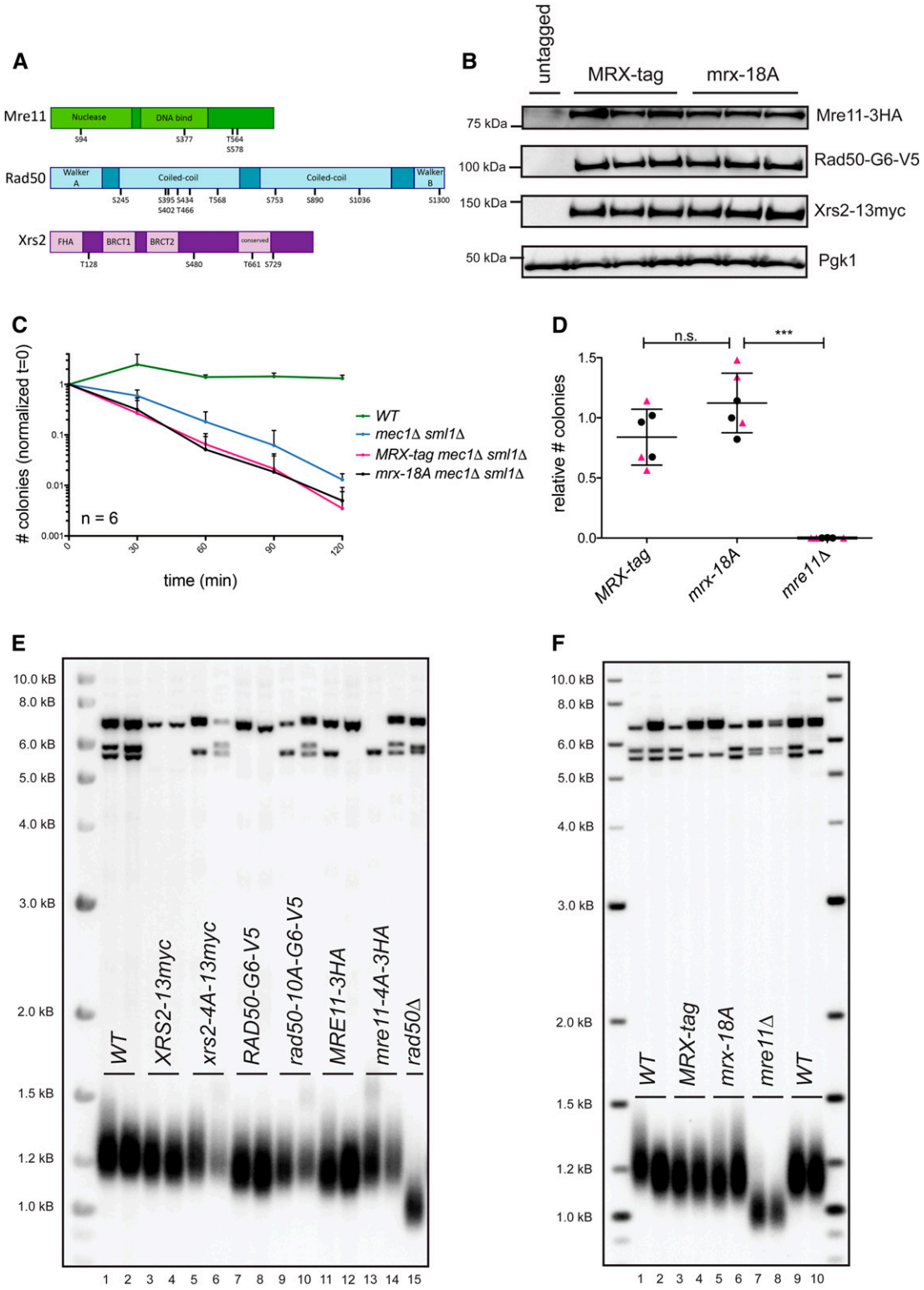

Figure 3 The mrx-18A S/T-Q mutant does not affect the DNA damage response, NHEJ, or telomere length. (A) Domain structure of the MRX complex indicating location of S/T-Q motifs with data from Lee *et al.* 2013; Shima *et al.* 2005; Becker *et al.* 2006 and are consistent with NCBI annotation (Mre11: BAA02017.1, Rad50: CAA65494, Xrs2: AAA35220.(1). S/T-Q motifs are indicated with a bar and the corresponding S or T residue number. (B) Western blots examining stability of the MRX complex in *MRX-tag* and *mrx-18A* strains. Quantitation was performed relative to Pgk1 loading control and normalized to the second lane of the Western blot. The average relative protein level in MRX-tag cells was 1.11 for Mre11-3HA, 1.07 for Rad50-G6-V5, and 0.88 for Xrs2-13myc. The average protein level in mrx-18A cells was 1.01 for mre11-4A-3HA, 1.02 for rad50-10A-G6-V5, and 0.69 for xrs2-4A-13myc. By unpaired two-tailed Student *t*-test there was no significant difference between the tagged and mutant-tagged protein for any MRX complex component. Strains used in the Western blot are derived from yRK79, yRK80, yRK81, and yRK83. (C) Proportion of colonies on cells treated with 0.01%

*mec1*Δ lethality by *TEL1-hy909* is MRX-dependent (Figure S8). This was also true for *TEL1-hy909 mec1*Δ *rad50*Δ and *TEL1-hy909 mec1*Δ *xrs2*Δ (not shown).

We next examined telomere length in *TEL1-hy909 mre11*Δ, *TEL1-hy909 rad50*Δ, and *TEL1-hy909 xrs2*Δ double mutants and found that, surprisingly, in all three cases the double mutants had long telomeres, similar to *TEL1-hy909* alone (Figure 4B). This indicates that, unlike the DNA damage response, MRX is not epistatic to Tel1 for telomere length. Because this result differs from previous findings, we repeated the experiment in the strain background (W303) used in the previous study (Baldo *et al.* 2008). In this separate analysis, again all three independently derived double mutants *TEL1-hy909 mre11*Δ, *TEL1-hy909 rad50*Δ, and *TEL1-hy909 xrs2*Δ showed long telomeres consistent with our initial findings (Figure S9A). We also passaged *TEL1-hy909 xrs2*Δ for 120 population doublings to see if shortening might occur with further divisions. Instead, we found telomeres elongated further with passaging (Figure S9B). This was also true for *TEL1-hy909 mre11*Δ and *TEL1-hy909 rad50*Δ cells in the BY and W303 backgrounds (Figure S9C and not shown). These data suggest that MRX is not required downstream of Tel1-hy909 to carry out telomere elongation.

To further investigate the requirement of nuclease activity at the telomere, we tested the epistatic relationship between *TEL1-hy909* and deletion of Sae2 (CtIP), which stimulates Mre11 (Lengsfeld *et al.* 2007), or Exo1, which extends Mre11-initiated resection at a double-strand break (Garcia *et al.* 2011) and has been suggested to play a role in telomere processing (Moreau *et al.* 2001). We generated diploid strains that were heterozygous for *TEL1/TEL1-hy909*, *MRE11/mre11*Δ, and *EXO1/exo1*Δ, and diploid strains that were heterozygous for *TEL1/TEL1-hy909*, *MRE11/mre11*Δ, and *SAE2/sae2*Δ. Both the double mutant *TEL1-hy909 exo1*Δ and the triple mutant *TEL1-hy909 mre11*Δ *exo1*Δ had long telomeres similar to *TEL1-hy909* alone (Figure 4C, compare lanes 5 and 6 to lanes 7 and 8 and to lanes 11 and 12). We found a similar result with *sae2*Δ: both the double mutant *TEL1-hy909 sae2*Δ and the triple mutant *TEL1-hy909 mre11*Δ *sae2*Δ cells had long telomeres, similar to *TEL1-hy909* alone (Figure 4D, compare lanes 5 and 6 to lanes 7 and 8 and to lanes 11 and 12). As compared to *TEL1-hy909* cells, which exhibit a single, continuous telomere distribution, we noted that many segregants derived from these heterozygous diploids had multimodal telomere length distributions. Because the multimodal distribution was present in wild-type haploids, in addition to haploids lacking Mre11, Exo1, and/or Sae2, we attribute this to an increase in telomere or subtelomere recombination during meiosis. The long telomeres in both triple mutants indicate that neither Exo1 nor Sae2 is compensating for the loss of Mre11. These data support the conclusion that telomere resection by Mre11/Sae2 or Exo1 is not required for telomere elongation.

rad50S activates Tel1 for telomere length maintenance

The ability of Tel1-hy909 to generate long telomeres in the absence of MRX suggests that this hypermorph is constitutively active as it does not require activation by MRX. As an independent approach to determine whether MRX is only required upstream of Tel1 in telomere length regulation, we performed a similar epistasis experiment using *tel1*Δ and a previously identified MRX complex mutant, *rad50S* (Alani *et al.* 1990). rad50S produces a long telomere phenotype that has been attributed to increased Tel1 activation (Kironmai and Muniyappa 1997). *rad50S* mutants are reported to have a sporulation defect (Usui *et al.* 2001), therefore we initiated these experiments in haploid cells. We used CRISPR/Cas9 to knock-in the *rad50S* allele at the endogenous *RAD50* locus (Anand *et al.* 2017). Elongated telomeres were observed after cells were passaged for ~120 population doublings (Figure 5A). In these haploids, we subsequently introduced a *tel1*Δ or *TEL1-hy909* allele at the *TEL1* locus. As a control, parallel strains were generated where a *mre11*Δ allele was introduced at the *MRE11* locus. Without Mre11, rad50S should not be able function in the MRX complex and the hypermorph activity will not be observed. Telomere shortening was observed in *rad50S mre11*Δ cells, as expected (Figure 5A). *rad50S tel1*Δ double mutants showed short telomeres, similar in length to *tel1*Δ (Figure 5A), indicating that Tel1 is required for the telomere elongation seen in *rad50S* cells. We also found that rad50S *TEL1-hy909* had very long telomeres, similar to *TEL1-hy909* (Figure 5B) and consistent with both mutant alleles acting in the same pathway. Our data indicate that MRX activates Tel1 but does not contribute to processing of telomeres to allow telomere lengthening

MMS over 120 min (see *Materials and Methods*). Proportion is calculated as the number of colonies at a given time point relative to the number of colonies for that genotype at $t = 0$. The average and SE of the mean of six technical replicates is plotted for each genotype with error bars only going upward for clarity. Strains included are yRK114, yRK128, yRK104, and yRK92. (D) Plasmid end-joining assay results with three technical replicates for each of two biological replicates (see *Materials and Methods*). Black circles correspond to the first biological replicate and pink triangles correspond to the second biological replicate. An unpaired two-tailed Student's *t*-test comparing *MRX-tag* to *mrx-18A* had a *P*-value = 0.068 and was not significant (n.s.). Comparison of *mrx-18A* to *mre11Δ* had a *P*-value < 0.0001 (***). Strains included are segregants from yRK79, yRK80, yRK81, yRK83, and yRK5064. (E) Southern blot analysis of telomeres from strains with the indicated genotype. Two independent, haploid segregants are shown for each genotype. The *rad50Δ* haploid was yRK2024 and was passaged for 200 generations. All other genotypes were segregants of yRK3018, yRK35, or yRK36 and were not passaged. Additional biological replicates were assayed for each genotype: *WT*, $n = 12$; MRE11-*3HA*, $n = 6$; *mre11-4A-3HA*, $n = 6$; *RAD50-G6-V5*, $n = 6$; *rad50-10A-G6-V5*, $n = 6$; *XRS2-13myc*, $n = 6$; *xrs2-4A-13myc*, $n = 4$. (F) Southern blot analysis of telomeres from strains with the indicated genotype. The median telomere lengths are reported in Figure S7A. The *mre11Δ* haploids were yRK1018 and yRK1019 and were passaged for ~200 population doublings. *WT*, *MRX-tag*, and *mrx-18A* haploids were segregants from yRK79, yRK80, yRK81, and yRK83. Additional biological replicates were assayed for each genotype: *WT*, $n = 12$; *MRX-tag*, $n = 6$; *mrx-18A*, $n = 8$.

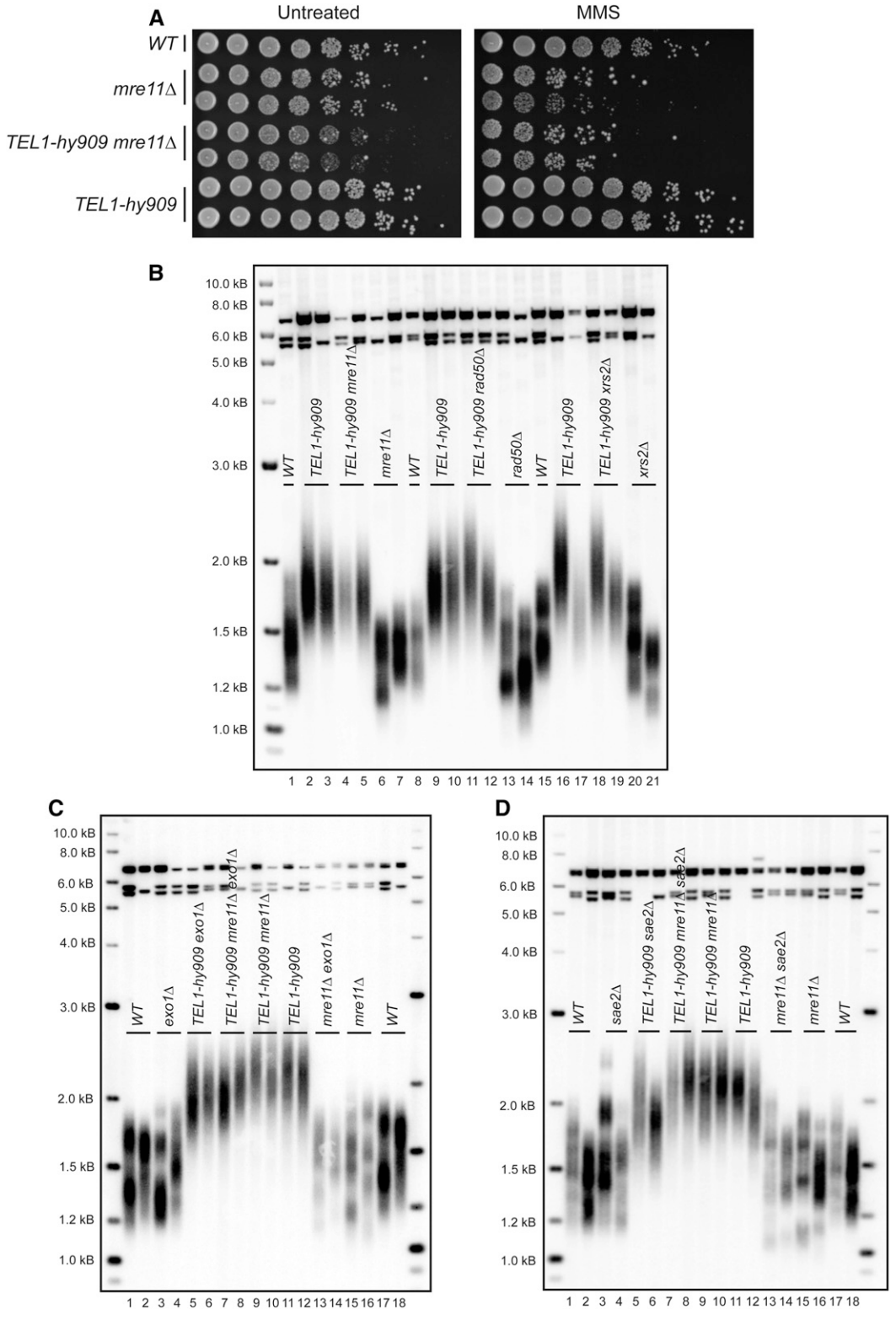

Figure 4 Tel1-hy909 requires the MRX complex for the DNA damage response but not for telomere elongation. (A) Yeast dilution series of untreated cells or cells treated with 0.02% MMS for 1 hr. The genotype is indicated to the left of the panels. To account for growth differences between the genotypes different amounts of cells were collected for the initial dilution. A total of 0.5 OD of cells were collected for *WT* and *TEL1-hy909*, 1.5 OD of cells were collected for *mre11Δ*, and 8.0 OD of cells were collected for *TEL1-hy909 mre11Δ*. Strains used in this assay were yRK114, yRK126, yRK128, yRK104, yRK141, yRK92, yRK93, and yRK122. (B–D) Southern blot analysis of telomeres from strains with the indicated genotype. Two independent, haploid segregants are shown for each genotype. (B) Segregants are from JHUy816, yRK79, yRK80, yRK81, and yRK83. Cells underwent minimal propagation before genomic DNA was prepared. Additional biological replicates were assayed for each genotype: *WT*, $n = 35$; *TEL1-hy909*, $n = 42$;

after Tel1 activation. In contrast, the MRX complex is critical downstream of Tel1 for the DNA damage response (Figure 6).

Discussion

Telomere elongation and DNA damage response are regulated through different mechanisms

We found that, in contrast to published models, the MRX complex is not required after Tel1 activation for telomere elongation. Our data suggest a new model in which Tel1 activation by MRX is sufficient for telomere length regulation but not for the DNA damage response (Figure 6). We note that studies of *mre11(ts)*, a temperature-sensitive, separation-of-function allele, also concluded that the MRX complex may play a different role in DNA damage and telomere length regulation (Chamankhah *et al.* 2000). Previous work has shown that Mec1 and Rad53 play a major role in the DNA damage response, while Tel1 plays a minor role acting through Rad53 and the MRX complex. In the DNA damage response, the MRX complex is thought to act both upstream and downstream of Tel1 (Usui *et al.* 2001; Paull 2015). MRX binds to double-strand breaks and recruits Tel1, activating its kinase activity. Previously, a parallel model for telomere length regulation suggested that MRX recruits and activates Tel1 at the telomere, then MRX processes telomere ends to promote telomerase elongation (Larrivee *et al.* 2004; Bonetti *et al.* 2009). In this model, Mec1 is considered secondary to Tel1 for telomere length regulation and its function was presumed to be redundant. In contrast, we show that Mec1 and Rad53 act in a separate, non-overlapping pathway from Tel1 for telomere length maintenance. Together these data demonstrate that the Tel1 and Mec1 pathways differ significantly for the DNA damage response and telomere length regulation.

Dysregulation of dNTP pools can mask telomere length phenotypes

The role of Mec1 in telomere length regulation has remained poorly understood, in part because of discrepancies in reported telomere length phenotypes. *mec1*Δ *sml1*Δ telomeres appear similar to wild type, while *mec1*Δ *crt1*Δ telomeres are shorter than wild type (Figure 1B). Both *sml1*Δ and *crt1*Δ suppress the lethality of *mec1*Δ through upregulation of different pathways that regulate nucleotide pools (Huang *et al.* 1998; Zhao *et al.* 1998). Several studies suggest that the increased telomere length in *mec1*Δ *sml1*Δ compared to *mec1* mutants is due to increased telomerase processivity with increased dGTP levels (Gupta *et al.* 2013). Recent work has suggested that, while both *sml1*Δ and *crt1*Δ increase nucleotide pools, they each have different effects on the specific ratio of dGTP to other dNTPs (Maicher *et al.* 2017). Because dGTP is limiting for telomerase processivity *in vitro* (Greider and Blackburn 1987; Hammond and Cech 1997), it was proposed that an increased dGTP/dNTP ratio would elongate telomeres (Maicher *et al.* 2017). However, we note that increased dNTP levels are not sufficient to lengthen telomeres, as *sml1*Δ and *crt1*Δ mutants do not show increased telomere length on their own. Also, *crt1*Δ does not lengthen telomeres in either a *tel1*Δ or *mec1*Δ background (Figure 1B). Therefore, while changes in dNTP pools in *mec1*Δ *sml1*Δ cells may mask telomere length phenotypes (Longhese *et al.* 2000), the data are not consistent with altered telomerase processivity as the mechanism.

Rad53 phosphorylation by Mec1 contributes to telomere length regulation

Previous work has shown that Tel1 or Mec1 phosphorylation of Rad53 is critical for the DNA damage response. Our data demonstrate an additional role for Rad53 phosphorylation in telomere length regulation. This phosphorylation is likely primarily performed by Mec1, as our data indicate that Rad53 is in the Mec1 telomere length pathway and previous work demonstrated that Mec1 phosphorylation of Rad53 is predominant in the DNA damage response (Usui *et al.* 2001). We cannot exclude the possibility that Tel1 phosphorylation of Rad53 contributes in a small way to telomere length regulation. However, the *TEL1-hy909* hypermorphic allele showed telomere elongation in the absence of Rad53 (Figure 2, C and D), suggesting that Tel1 does not require Rad53 for telomere length regulation. Our model suggests there are as yet unknown substrates that mediate the Tel1 effect on telomere length (Figure 6).

Rad53 is a critical mediator of Mec1 in telomere length regulation

The *TEL1-hy909* hypermorphic allele can rescue the lethality of *mec1*Δ, as shown previously (Baldo *et al.* 2008). However, we found that *TEL1-hy909* did not rescue *rad53*Δ lethality (Figure S2A). Rad53 is a substrate of both Tel1 and Mec1 (Sanchez *et al.* 1996; Smolka *et al.* 2007). Both *mec1*Δ and *rad53*Δ are thought to be lethal due to an inability to upregulate ribonucleotide reductases for DNA repair. *Tel1-hy909* has increased catalytic activity *in vitro* and is able to phosphorylate Rad53 more efficiently than Tel1 (Baldo *et al.* 2008). Tel1-hy909 likely rescues *mec1*Δ lethality because of its increased ability to activate Rad53. Our finding that *TEL1-hy909* cannot rescue *rad53*Δ places

TEL1-hy909 mre11Δ, *n* = 21; *mre11Δ*, *n* = 18; *TEL1-hy909 rad50Δ*, *n* = 18; *rad50Δ*, *n* = 15; *TEL1-hy909 xrs2Δ*, *n* = 4; *xrs2Δ*, *n* = 4. (C) Segregants are from yRK5150 and yRK5151. Cells underwent minimal propagation before genomic DNA was prepared. Additional biological replicates were assayed for each genotype: *WT*, *n* = 35; *exo1Δ*, *n* = 4; *TEL1-hy909 exo1Δ*, *n* = 4; *TEL1-hy909 exo1Δ mre11Δ*, *n* = 4; *TEL1-hy909 mre11Δ*, *n* = 21; *TEL1-hy909*, *n* = 42; *mre11Δ exo1Δ*, *n* = 2; *mre11Δ*, *n* = 18. (D) Segregants are from yRK5152 and yRK5153. Cells underwent minimal propagation before genomic DNA was prepared. Additional biological replicates were assayed for each genotype: *WT*, *n* = 25; *sae2Δ*, *n* = 6; *TEL1-hy909 sae2Δ*, *n* = 6; *TEL1-hy909 mre11Δ sae2Δ*, *n* = 4; *TEL1-hy909 mre11Δ*, *n* = 21; *TEL1-hy909*, *n* = 42; *mre11Δ sae2Δ*, *n* = 2; *mre11Δ*, *n* = 18.

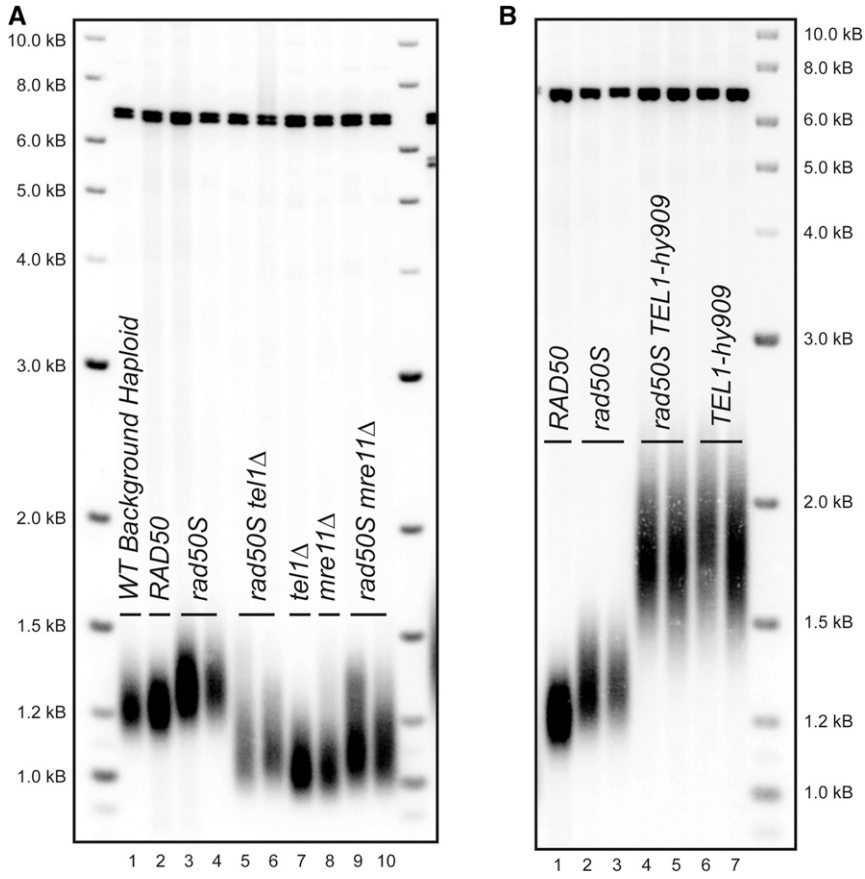

Figure 5 rad50S telomere elongation is dependent on Tel1. (A and B) CRISPR/Cas9 was used to knock-in the *rad50S* allele into a wild-type haploid strain (yRK114). A transformant that was not edited at the *RAD50* locus but was transformed with the Cas9 plasmid was used as a control and is referred to as *RAD50* (A, lane 2). Both *RAD50* and *rad50S* transformants were passaged on solid media for ~120 population doublings (see A, lanes 2–4, yRK2112-5, yRK2113-5, and yRK2116-5). *rad50S* or *RAD50* cells were transformed to introduce *tel1Δ*, *mre11Δ* (A, lanes 5–10), or *TEL1-hy909* (B, lanes 4–7). Cells were passaged on solid media for ~120 population doublings. The strains used were yRK2118-5, yRK2120-5, yRK2121-5, yRK2122-5, yRK2123-5, yRK2124-5, yRK2125-5, yRK2126-5, yRK2127-5, and yRK2128-5. Biological replicates were assayed for each genotype: *rad50S*, $n = 5$; *rad50S tel1Δ*, $n = 2$; *tel1Δ*, $n = 3$; *mre11Δ*, $n = 1$; *rad50S mre11Δ*, $n = 2$; *rad50S TEL1-hy909*, $n = 2$; *TEL1-hy909*, $n = 2$.

Rad53 as the critical mediator of Mec1. Mec1 loss can be compensated for by *Tel1-hy909*. but this hypermorph cannot compensate for loss of Rad53.

The *TEL1-hy909* allele is dominant as shown previously in the DNA damage response (Baldo *et al.* 2008) and as we saw in telomere length regulation (Figure S4B). While we cannot rule out that this allele has altered function other than increased kinase activity, those functions are likely limited to the Tel1 and Mec1 pathways since the *MRX* complex is epistatic to *TEL1-hy909* in the DNA damage response. *TEL1-hy909 mre11*Δ cells were just as sensitive as *mre11*Δ to MMS challenge (Figure 4A). This was also true for *TEL1-hy909 rad50*Δ and *TEL1-hy909 xrs2*Δ (data not shown). We unexpectedly found that *TEL1-hy909 mec1*Δ *mre11*Δ is lethal while *TEL1-hy909 mec1*Δ is viable (Figure S8). It is unclear why the *TEL1-hy909* rescue of *mec1*Δ viability is *MRX*-dependent. Taken together, our data suggest that the primary effect of the point mutations in *TEL1-hy909* allele is to make the kinase constitutively active.

MRX complex phosphorylation by Tel1/Mec1 on S/T-Q sites is not required for DNA damage response, NHEJ, or telomere length regulation

Multiple studies have reported that Tel1/Mec1-dependent phosphorylation of the MRX complex occurs in response to DNA damage. Thus, were surprised to find that the mrx-18A mutant did not have a DNA damage response phenotype or affect NHEJ (Figure 3). While phosphoproteomic experiments have identified Tel1/Mec1-dependent phosphorylation sites that are not on S/T-Q motifs, these are thought to be due to downstream kinases and are considered indirect targets of Tel1/Mec1 (Bastos de Oliveira *et al.* 2015). We further found that there was no effect of the mrx-18A mutant on telomere length, suggesting that MRX is not the substrate that mediates the Tel1 pathway of telomere length regulation.

Telomere elongation can occur in the absence of MRX complex

Our finding that Tel1-hy909 telomere elongation can occur in the absence of the MRX complex indicates that telomere elongation is possible without telomere end processing by MRX. Further, this indicates that the Tel1-hy909 hypermorph has bypassed the need to interact with MRX for its activation, and that the point mutations in the *TEL1-hy909* allele promote constitutive catalytic activity. This finding, combined with the fact that the mrx-18A mutant has no telomere length defect, suggest that Tel1 does not require MRX for telomere length regulation after it is activated. Models have proposed that telomere end processing is similar to double-strand-break end processing (Nugent *et al.* 1998; Tsukamoto *et al.* 2001; Larrivee *et al.* 2004; Viscardi *et al.* 2007; Bonetti *et al.* 2009; Pfeiffer and Lingner 2013).

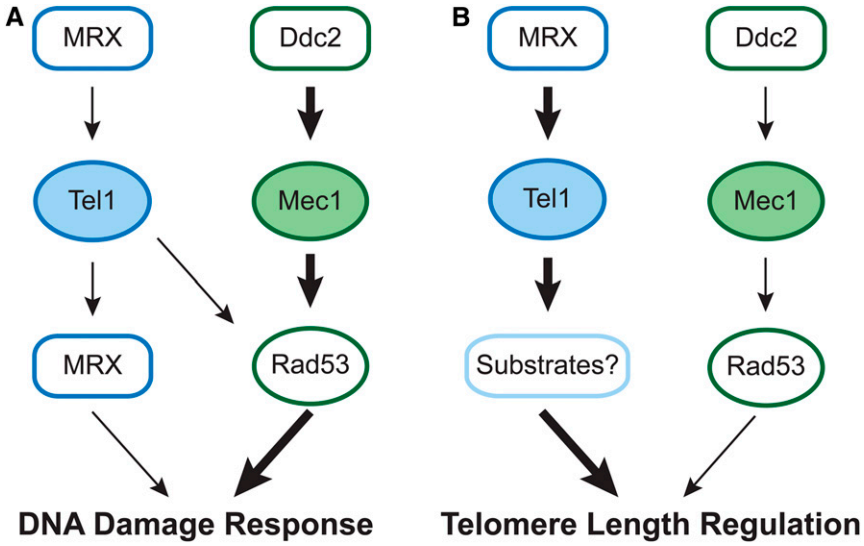

Figure 6 Tel1 regulates telomere length in a pathway distinct from the DNA damage response. Diagram demonstrating the distinctions between Tel1 pathways in the DNA damage response and telomere length regulation. (A) The DNA damage response is most strongly regulated by Mec1 and Rad53 as indicated with the bold arrows, although Tel1 signaling through Rad53 and MRX plays a role. The MRX complex is both upstream and downstream of Tel1 in the DNA damage response. (B) For telomere length regulation, Tel1 does not require MRX after activation and Rad53 does not plan a role in the Tel1 telomere length regulation pathway. The Tel1/MRX pathway plays the major role in telomere length compared to a minor role of Mec1/Rad53 pathway.

At a double-strand break, Ku binds to the DNA ends and then MRX recruitment allows end processing to produce substrates for either homology-directed repair or NHEJ. For homology-directed repair, Mre11 interacts with Sae2 to produce a 3′ overhang, by first endonuclease cleavage of the strand with a 5′ end near the break, followed by Mre11 3′ to 5′ exonuclease activity to remove the short region of double strand DNA and thus generate a 3′ overhang (Paull 2018). Exo1 then can extend the 3′ overhang through its 5′ to 3′ exonuclease function (Garcia *et al.* 2011).

Several lines of evidence suggest that these end processing events are not required for telomere elongation by telomerase. Mre11 nuclease dead (*mre11-ND*) mutants have previously been shown to have no effect on telomere length (Moreau *et al.* 1999; Tsukamoto *et al.* 2001). Deletion of *SAE2* or *EXO1* do not affect telomere length, suggesting that they are not essential for telomere end processing to allow elongation (Bonetti *et al.* 2009). It was shown that *sae2*Δ *sgs1*Δ generated by transformation of haploid cells have short telomeres (Bonetti *et al.* 2009). However, this telomere shortening effect was later attributed to suppressor mutations arising in *YKU70* and not because of *sae2*Δ *sgs1*Δ (Mimitou and Symington 2010; Hardy *et al.* 2014). Exo1 can resect a DNA break in the absence of Mre11, although less efficiently (Cejka 2015). However, we observed that *Tel1-hy909* was able to elongate telomeres in the absence of both Exo1 and Mre11 (Figure 4C) and overexpression of Exo1 does not rescue *mre11*Δ short telomeres (Chamankhah *et al.* 2000). Exo1 has been demonstrated to contribute to telomerase-independent telomere length regulation and in resecting deprotected telomeres (Bertuch and Lundblad 2004); however, a role in telomerase mediated telomere elongation has not been described to our knowledge. Together these data demonstrate that Mre11, Sae2, and Exo1 nuclease activity are not required for telomerase-dependent telomere length regulation.

MRX acts upstream of Tel1 for telomere length regulation

Our data support previous studies that place MRX action upstream of Tel1 but also suggest that for telomere length regulation MRX is not required downstream. First, the mutants in MRX that decrease telomere length are those that decrease the MRX complex interaction with Tel1 (*i.e.*, Xrs2 C-terminal truncation) (Nakada *et al.* 2003a; Ma and Greider 2009). Second, MRX mutants that decrease the catalytic functions of the complex are required for the DNA damage response, but not for telomere length regulation. For example, alleles of Mre11 that lack nuclease function do not show a telomere length phenotype (Moreau *et al.* 1999; Tsukamoto *et al.* 2001) but do inhibit the DNA damage response (Buis *et al.* 2008). Taken together with our evidence that *TEL1-hy909* is epistatic to MRX components, we conclude that cells with deletions of MRX complex components have short telomeres because of the reduction in Tel1 activation, and not because the cell lacks the resection functions.

Our finding that MRX is not required downstream of Tel1 for telomere elongation has important implications for telomere elongation models. Most models suggest that after replication of the telomere, the leading strand telomere is processed by a nuclease before telomerase can elongate it. The presumption that leading strand replication leaves a blunt end that requires processing is an assumption that has not been directly tested (Lingner and Cech 1998; Pfeiffer and Lingner 2013). In contrast to those models, our data suggest telomerase can efficiently elongate telomeres without end processing by MRX, Sae2, or Exo1. This suggests that telomerase may extend existing 3′ overhangs at the telomere. Tel1(ATM) and the MRX(N) complex are thought to function by similar mechanisms in *S. cerevisiae* and mammalian cells (Oh and Symington 2018; Paull 2018). Therefore, the data presented here suggest that

we should rethink the requirements for telomere resection preceding telomere elongation broadly across all organisms.

Acknowledgments

We thank Rini Mayangsuri for technical assistance with this work. We thank Brendan Cormack, Geraldine Seydoux, the Greider Laboratory, and the Armanios Laboratory for critical reading of the manuscript and helpful discussions. This work was supported by Bloomberg Distinguished Professorship (to C.W.G.) and the Turock Fellowship (to R.K.).

Author contributions: study conception: C.W.G. and R.K.; methodology: R.K. and C.W.G.; investigation and acquisition of data: R.K. and C.J.C.; supervision: C.W.G.; formal analysis and interpretation of data: R.K. and C.W.G.; validation: R.K. and C.J.C.; visualization: R.K.; data curation: R.K.; funding acquisition: C.W.G.; drafting of manuscript: R.K. and C.W.G.; critical revision: R.K., C.C., and C.W.G.

Literature Cited

Alani, E., R. Padmore, and N. Kleckner, 1990 Analysis of wild-type and rad50 mutants of yeast suggests an intimate relationship between meiotic chromosome synapsis and recombination. Cell 61: 419–436. https://doi.org/10.1016/0092-8674(90)90524-I

Albuquerque, C. P., M. B. Smolka, S. H. Payne, V. Bafna, J. Eng *et al.*, 2008 A multidimensional chromatography technology for in-depth phosphoproteome analysis. Mol. Cell. Proteomics 7: 1389–1396. https://doi.org/10.1074/mcp.M700468-MCP200

Anand, R., G. Memisoglu and J. Haber, 2017 Cas9-mediated gene editing in *Saccharomyces cerevisiae*. Protoc. Exch. https://doi.org/10.1038/protex.2017.021a

Armanios, M., and E. H. Blackburn, 2012 The telomere syndromes. Nat. Rev. Genet. 13: 693–704 [corrigenda: Nat. Rev. Genet. 14: 235 (2013)]. https://doi.org/10.1038/nrg3246

Arora, S., R. A. Deshpande, M. Budd, J. Campbell, A. Revere *et al.*, 2017 Genetic separation of Sae2 nuclease activity from Mre11 nuclease functions in budding yeast. Mol. Cell. Biol. 37: e00156-17. https://doi.org/10.1128/MCB.00156-17

Bähler, J., J. Q. Wu, M. S. Longtine, N. G. Shah, A. McKenzie, 111 *et al.*, 1998 Heterologous modules for efficient and versatile PCR-based gene targeting in *Schizosaccharomyces pombe*. Yeast 14: 943–951. https://doi.org/10.1002/(SICI)1097-0061(199807)14:10<943::AID-YEA292>3.0.CO;2-Y

Baldo, V., V. Testoni, G. Lucchini, and M. P. Longhese, 2008 Dominant *TEL1-hy* mutations compensate for Mec1 lack of functions in the DNA damage response. Mol. Cell. Biol. 28: 358–375. https://doi.org/10.1128/MCB.01214-07

Bastos de Oliveira, F. M., D. Kim, J. R. Cussiol, J. Das, M. C. Jeong *et al.*, 2015 Phosphoproteomics reveals distinct modes of Mec1/ATR signaling during DNA replication. Mol. Cell 57: 1124–1132 (erratum: Mol. Cell 57: 1124–1132). https://doi.org/10.1016/j.molcel.2015.01.043

Becker, E., V. Meyer, H. Madaoui, and R. Guerois, 2006 Detection of a tandem BRCT in Nbs1 and Xrs2 with functional implications in the DNA damage response. Bioinformatics 22: 1289–1292. https://doi.org/10.1093/bioinformatics/btl075

Bertuch, A. A., and V. Lundblad, 2004 *EXO1* contributes to telomere maintenance in both telomerase-proficient and telomerase-deficient *Saccharomyces cerevisiae*. Genetics 166: 1651–1659. https://doi.org/10.1534/genetics.166.4.1651

Bonetti, D., M. Martina, M. Clerici, G. Lucchini, and M. P. Longhese, 2009 Multiple pathways regulate 3′ overhang generation at *S. cerevisiae telomeres*. Mol. Cell 35: 70–81. https://doi.org/10.1016/j.molcel.2009.05.015

Boulton, S. J., and S. P. Jackson, 1996 Identification of a *Saccharomyces cerevisiae* Ku80 homologue: roles in DNA double strand break rejoining and in telomeric maintenance. Nucleic Acids Res. 24: 4639–4648. https://doi.org/10.1093/nar/24.23.4639

Buis, J., Y. Wu, Y. Deng, J. Leddon, G. Westfield *et al.*, 2008 Mre11 nuclease activity has essential roles in DNA repair and genomic stability distinct from ATM activation. Cell 135: 85–96. https://doi.org/10.1016/j.cell.2008.08.015

Cejka, P., 2015 DNA end resection: nucleases team up with the right partners to initiate homologous recombination. J. Biol. Chem. 290: 22931–22938. https://doi.org/10.1074/jbc.R115.675942

Chamankhah, M., T. Fontanie, and W. Xiao, 2000 The *Saccharomyces cerevisiae mre11(ts)* allele confers a separation of DNA repair and telomere maintenance functions. Genetics 155: 569–576.

D'Amours, D., and S. P. Jackson, 2001 The yeast Xrs2 complex functions in S phase checkpoint regulation. Genes Dev. 15: 2238–2249. https://doi.org/10.1101/gad.208701

de Lange, T., 2018 Shelterin-mediated telomere protection. Annu. Rev. Genet. 52: 223–247. https://doi.org/10.1146/annurev-genet-032918-021921

Doench, J. G., N. Fusi, M. Sullender, M. Hegde, E. W. Vaimberg *et al.*, 2016 Optimized sgRNA design to maximize activity and minimize off-target effects of CRISPR-Cas9. Nat. Biotechnol. 34: 184–191. https://doi.org/10.1038/nbt.3437

Garcia, V., S. E. Phelps, S. Gray, and M. J. Neale, 2011 Bidirectional resection of DNA double-strand breaks by Mre11 and Exo1. Nature 479: 241–244. https://doi.org/10.1038/nature10515

Gibson, D. G., 2011 Enzymatic assembly of overlapping DNA fragments. Methods Enzymol. 498: 349–361. https://doi.org/10.1016/B978-0-12-385120-8.00015-2

Green, M., and J. Sambrook, 2012 *Molecular cloning: a laboratory manual*

Greider, C. W., 1999 Telomerase activation: one step on the road to cancer? Trends Genet. 15: 109–112. https://doi.org/10.1016/S0168-9525(98)01681-3

Greider, C. W., and E. H. Blackburn, 1987 The telomere terminal transferase of *Tetrahymena* is a ribonucleoprotein enzyme with two kinds of primer specificity. Cell 51: 887–898. https://doi.org/10.1016/0092-8674(87)90576-9

Gupta, A., S. Sharma, P. Reichenbach, L. Marjavaara, A. K. Nilsson *et al.*, 2013 Telomere length homeostasis responds to changes in intracellular dNTP pools. Genetics 193: 1095–1105. https://doi.org/10.1534/genetics.112.149120

Hammond, P. W., and T. R. Cech, 1997 dGTP-dependent processivity and possible template switching of euplotes telomerase. Nucleic Acids Res. 25: 3698–3704. https://doi.org/10.1093/nar/25.18.3698

Hardy, J., D. Churikov, V. Geli, and M. N. Simon, 2014 Sgs1 and Sae2 promote telomere replication by limiting accumulation of ssDNA. Nat. Commun. 5: 5004. https://doi.org/10.1038/ncomms6004

Hector, R. E., R. L. Shtofman, A. Ray, B. R. Chen, T. Nyun *et al.*, 2007 Tel1p preferentially associates with short telomeres to stimulate their elongation. Mol. Cell 27: 851–858. https://doi.org/10.1016/j.molcel.2007.08.007

Huang, M., Z. Zhou, and S. J. Elledge, 1998 The DNA replication and damage checkpoint pathways induce transcription by inhibition of the Crt1 repressor. Cell 94: 595–605. https://doi.org/10.1016/S0092-8674(00)81601-3

Kaizer, H., C. J. Connelly, K. Bettridge, C. Viggiani, and C. W. Greider, 2015 Regulation of telomere length requires a conserved N-terminal Domain of Rif2 in *Saccharomyces cerevisiae*. Genetics 201: 573–586. https://doi.org/10.1534/genetics.115.177899

Kim, S. T., D. S. Lim, C. E. Canman, and M. B. Kastan, 1999 Substrate specificities and identification of putative substrates of ATM kinase family members. J. Biol. Chem. 274: 37538–37543. https://doi.org/10.1074/jbc.274.53.37538

Kironmai, K. M., and K. Muniyappa, 1997 Alteration of telomeric sequences and senescence caused by mutations in *RAD50* of *Saccharomyces cerevisiae*. Genes Cells 2: 443–455. https://doi.org/10.1046/j.1365-2443.1997.1330331.x

Larrivee, M., C. LeBel, and R. J. Wellinger, 2004 The generation of proper constitutive G-tails on yeast telomeres is dependent on the MRX complex. Genes Dev. 18: 1391–1396. https://doi.org/10.1101/gad.1199404

Lavin, M. F., S. Kozlov, M. Gatei, and A. W. Kijas, 2015 ATM-dependent phosphorylation of all three members of the MRN complex: from sensor to adaptor. Biomolecules 5: 2877–2902. https://doi.org/10.3390/biom5042877

Lee, J. H., M. R. Mand, R. A. Deshpande, E. Kinoshita, S. H. Yang *et al*., 2013 Ataxia telangiectasia-mutated (ATM) kinase activity is regulated by ATP-driven conformational changes in the Mre11/Rad50/Nbs1 (MRN) complex. J. Biol. Chem. 288: 12840–12851. https://doi.org/10.1074/jbc.M113.460378

Lee, S.-J., M. F. Schwartz, J. K. Duong, and D. F. Stern, 2003 Rad53 phosphorylation site clusters are important for Rad53 regulation and signaling. Mol. Cell. Biol. 23: 6300–6314. https://doi.org/10.1128/MCB.23.17.6300-6314.2003

Lee, S. S., C. Bohrson, A. M. Pike, S. J. Wheelan, and C. W. Greider, 2015 ATM kinase is required for telomere elongation in mouse and human cells. Cell Reports 13: 1623–1632. https://doi.org/10.1016/j.celrep.2015.10.035

Lengsfeld, B. M., A. J. Rattray, V. Bhaskara, R. Ghirlando, and T. T. Paull, 2007 Sae2 is an endonuclease that processes hairpin DNA cooperatively with the Mre11/Rad50/Xrs2 complex. Mol. Cell 28: 638–651. https://doi.org/10.1016/j.molcel.2007.11.001

Lingner, J., and T. R. Cech, 1998 Telomerase and chromosome end maintenance. Curr. Opin. Genet. Dev. 8: 226–232. https://doi.org/10.1016/S0959-437X(98)80145-7

Link, A. J., and J. LaBaer, 2011 Trichloroacetic acid (TCA) precipitation of proteins. Cold Spring Harb. Protoc. 2011: 993–994. https://doi.org/10.1101/pdb.prot5651

Longhese, M. P., V. Paciotti, H. Neecke, and G. Lucchini, 2000 Checkpoint proteins influence telomeric silencing and length maintenance in budding yeast. Genetics 155: 1577–1591.

Ma, Y., and C. W. Greider, 2009 Kinase-independent functions of *TEL1* in telomere maintenance. Mol. Cell. Biol. 29: 5193–5202. https://doi.org/10.1128/MCB.01896-08

Maicher, A., I. Gazy, S. Sharma, L. Marjavaara, G. Grinberg *et al*., 2017 Rnr1, but not Rnr3, facilitates the sustained telomerase-dependent elongation of telomeres. PLoS Genet. 13: e1007082. https://doi.org/10.1371/journal.pgen.1007082

Mallory, J. C., V. I. Bashkirov, K. M. Trujillo, J. A. Solinger, M. Dominska *et al*., 2003 Amino acid changes in Xrs2p, Dun1p, and Rfa2p that remove the preferred targets of the ATM family of protein kinases do not affect DNA repair or telomere length in *Saccharomyces cerevisiae*. DNA Repair (Amst.) 2: 1041–1064. https://doi.org/10.1016/S1568-7864(03)00115-0

Mimitou, E. P., and L. S. Symington, 2010 Ku prevents Exo1 and Sgs1-dependent resection of DNA ends in the absence of a functional MRX complex or Sae2. EMBO J. 29: 3358–3369. https://doi.org/10.1038/emboj.2010.193

Moore, J. K., and J. E. Haber, 1996 Cell cycle and genetic requirements of two pathways of nonhomologous end-joining repair of double-strand breaks in *Saccharomyces cerevisiae*. Mol. Cell. Biol. 16: 2164–2173. https://doi.org/10.1128/MCB.16.5.2164

Moreau, S., H. R. Ferguson, and L. S. Symington, 1999 The nuclease activity of Mre11 is required for meiosis but not for mating type switching, end joiningor telomere maintenance. Mol. Cell. Biol. 19: 556–566. https://doi.org/10.1128/MCB.19.1.556

Moreau, S., E. A. Morgan, and L. S. Symington, 2001 Overlapping functions of the *Saccharomyces cerevisiae* Mre11, Exo1 and Rad27 nucleases in DNA metabolism. Genetics 159: 1423–1433.

Morrow, D. M., D. A. Tagle, Y. Shiloh, F. S. Collins, and P. Hieter, 1995 *TEL1*, an *S. cerevisiae* homolog of the human gene mutated in ataxia telangiectasia, is functionally related to the yeast checkpoint gene *MEC1*. Cell 82: 831–840. https://doi.org/10.1016/0092-8674(95)90480-8

Nakada, D., K. Matsumoto, and K. Sugimoto, 2003a ATM-related Tel1 associates with double-strand breaks through an Xrs2-dependent mechanism. Genes Dev. 17: 1957–1962. https://doi.org/10.1101/gad.1099003

Nakada, D., T. Shimomura, K. Matsumoto, and K. Sugimoto, 2003b The ATM-related Tel1 protein of *Saccharomyces cerevisiae* controls a checkpoint response following phleomycin treatment. Nucleic Acids Res. 31: 1715–1724. https://doi.org/10.1093/nar/gkg252

Nugent, C. I., G. Bosco, L. O. Ross, S. K. Evans, A. P. Salinger *et al*., 1998 Telomere maintenance is dependent on activities required for end repair of double-strand breaks. Curr. Biol. 8: 657–660. https://doi.org/10.1016/S0960-9822(98)70253-2

Oh, J., and L. S. Symington, 2018 Role of the Mre11 complex in preserving genome integrity. Genes (Basel) 9: E589. https://doi.org/10.3390/genes9120589

Paull, T. T., 2015 Mechanisms of ATM activation. Annu. Rev. Biochem. 84: 711–738. https://doi.org/10.1146/annurev-biochem-060614-034335

Paull, T. T., 2018 20 Years of Mre11 biology: No end in sight. Mol. Cell 71: 419–427. https://doi.org/10.1016/j.molcel.2018.06.033

Pfeiffer, V., and J. Lingner, 2013 Replication of telomeres and the regulation of telomerase. Cold Spring Harb. Perspect. Biol. 5: a010405. https://doi.org/10.1101/cshperspect.a010405

Ritchie, K. B., J. C. Mallory, and T. D. Petes, 1999 Interactions of *TLC1* (which encodes the RNA subunit of telomerase), *TEL1*, and *MEC1* in regulating telomere length in the yeast *Saccharomyces cerevisiae*. Mol. Cell. Biol. 19: 6065–6075. https://doi.org/10.1128/MCB.19.9.6065

Sabourin, M., C. T. Tuzon, and V. A. Zakian, 2007 Telomerase and Tel1p preferentially associate with short telomeres in *S. cerevisiae*. Mol. Cell 27: 550–561. https://doi.org/10.1016/j.molcel.2007.07.016

Sanchez, Y., B. A. Desany, W. J. Jones, Q. Liu, B. Wang *et al*., 1996 Regulation of *RAD53* by the *ATM*-like kinases *MEC1* and *TEL1* in yeast cell cycle checkpoint pathways. Science 271: 357–360. https://doi.org/10.1126/science.271.5247.357

Shampay, J., and E. H. Blackburn, 1988 Generation of telomere-length heterogeneity in *Saccharomyces cerevisiae*. Proc. Natl. Acad. Sci. USA 85: 534–538. https://doi.org/10.1073/pnas.85.2.534

Shima, H., M. Suzuki, and M. Shinohara, 2005 Isolation and characterization of novel *xrs2* mutations in *Saccharomyces cerevisiae*. Genetics 170: 71–85. https://doi.org/10.1534/genetics.104.037580

Sikorski, R. S., and J. D. Boeke, 1991 *In vitro* mutagenesis and plasmid shuffling: from cloned gene to mutant yeast. Methods Enzymol. 194: 302–318. https://doi.org/10.1016/0076-6879(91)94023-6

Smolka, M. B., C. P. Albuquerque, S. H. Chen, and H. Zhou, 2007 Proteome-wide identification of *in vivo* targets of DNA

damage checkpoint kinases. Proc. Natl. Acad. Sci. USA 104: 10364–10369. https://doi.org/10.1073/pnas.0701622104

Stanley, S. E., and M. Armanios, 2015 The short and long telomere syndromes: paired paradigms for molecular medicine. Curr. Opin. Genet. Dev. 33: 1–9. https://doi.org/10.1016/j.gde.2015.06.004

Tong, A. S., J. L. Stern, A. Sfeir, M. Kartawinata, T. de Lange *et al.*, 2015 ATM and ATR signaling regulate the recruitment of human telomerase to telomeres. Cell Reports 13: 1633–1646. https://doi.org/10.1016/j.celrep.2015.10.041

Tsukamoto, Y., A. K. Taggart, and V. A. Zakian, 2001 The role of the Mre11-Rad50-Xrs2 complex in telomerase- mediated lengthening of *Saccharomyces cerevisiae* telomeres. Curr. Biol. 11: 1328–1335. https://doi.org/10.1016/S0960-9822(01)00372-4

Usui, T., H. Ogawa, and J. H. Petrini, 2001 A DNA damage response pathway controlled by Tel1 and the Mre11 complex. Mol. Cell 7: 1255–1266. https://doi.org/10.1016/S1097-2765(01)00270-2

Viscardi, V., D. Bonetti, H. Cartagena-Lirola, G. Lucchini, and M. P. Longhese, 2007 MRX-dependent DNA damage response to short telomeres. Mol. Biol. Cell 18: 3047–3058. https://doi.org/10.1091/mbc.e07-03-0285

Zhao, X., E. G. Muller, and R. Rothstein, 1998 A suppressor of two essential checkpoint genes identifies a novel protein that negatively affects dNTP pools. Mol. Cell 2: 329–340. https://doi.org/10.1016/S1097-2765(00)80277-4

Communicating editor: J. Engebrecht